ADDIS ABABA UNIVERSITY
ADDIS ABABA INSTITUTE OF TECHNOLOGY
SCHOOL OF GRADUATE STUDIES

PERFORMANCE ANALYSIS AND RELIABLITY TESTING OF A CERAMIC BAKE WARE FOR AN ELECTRIC INJERA BAKING STOVE

A Thesis Submitted to the School of Graduate Studies of Addis Ababa University in Partial Fulfillment of the Requirements for the Degree of Masters of Science in Mechanical Engineering (Thermal Engineering Stream.)

By: Garedew Ambaw Tsige
Advisor: Dr.Ing Demiss Alemu

Addis Ababa, Ethiopia
April 2015

ADDIS ABABA UNIVERSITY

ADDIS ABABA INSTITUTE OF TECHNOLOGY

SCHOOL OF GRADUATE STUDIES

PERFORMANCE ANALYSIS AND RELIABLITY TESTING OF A CERAMIC BAKE WARE FOR AN ELECTRIC INJERA BAKING STOVE

Submitted By:

Garedew Ambaw	_____	_____
(Student)	Signature	Date

Approved By:

1. Dr. Ing. Demiss Alemu	_____	_____
(Thesis Advisor)	Signature	Date
2. Dr.Tesfayie Dama	_____	_____
(Internal Examiner)	Signature	Date
3. Dr.Ing Edessa Deribsa	_____	_____
(External Examiner)	Signature	Date
4. _____	_____	_____
(Dean of School)	Signature	Date

ACKNOWLEDGMENT

First I would like to express my deepest appreciation and thankfulness to my thesis Advisor Dr.Ing Demiss Alemu for his skillful knowledge, encouragement and supervisions that greatly helped me during the time of my thesis work.

Next my specials thanks goes to HAWASA TABOR CERAMICS PLC. Workers especially Ato Berhanu and Ato Eferem, for their help in the manufacturing of the mitad samples used for the test. I would also like to extend my thanks to the entire members of AAiT Mechanical engineering Department and work shop staff for their support in one way or the other during assembling the stove and taking experimental measurements of the laboratory model.

Even though there are many peoples who had a direct or indirect contribution to the present accomplishment; the efforts and motivation from my family and close relatives is worth to be mentioned, had it not been for your help and motivation it would have been too difficult even to start at the beginning.

Garedew Ambaw Tsige

April 2015, Addis Ababa

ABSTRACT

In this study, the suitability and reliability of a ceramic bake ware based electric stove (CBWBES) for injera baking application were assessed experimentally and a mathematical model of the coupled heat and mass transfer of the baking process was developed and solved using Finite Element (FE) method. MATLAB code was used to perform the FE analysis, which is then used to estimate the performance of the CBWBES for different numbers of baking cycles.

The FE model was first validated using experimental data obtained from field testing of the performance of the CBWBES. The reliability of the CBWBES was investigated for its thermal shock resistance by subjecting the mitad in cycles of baking, and heating and cooling tests from (180 to 210 ^{o}C). Regarding the suitability of the new ceramic mitad While; two injera baked at mitad top surface temperature of 210^{o}c Shows poor product quality formation 10 injera baked at a reduced temperature of 147 to 150^{o}c Shows its suitability for the intended application. The CBWBES passed 12 cycles ‘of injera baking and 6 heating and air cooling cycles without the occurrence of deep cracks in the body. The 10 injera produced before the advent of the cracks was in good quality, with an excellent bottom crest formation and porous top surface structure. The total energy intensity of the new CBWBES was calculated and becomes 1.96 MJ/kg.; which is comparably close to the value of the conventional clay stove, which is 1.79 MJ/kg. The higher thermal inertia of the new CBWBES yields longer heat up times and longer times to recover the baking surface temperature once injera is baked; this was mainly attributed to the increased thickness of the bake ware used for the present test.

The heat up time obtained experimentally closely matched with the simulation result with an error of less than 10 %., and the simulation shows about 82 % efficiency can be realizable by reducing the thickness to 8mm for 20 cycles of injera baking, even though the absence of suitable production process in manufacturing the ceramic mitad affects its quality for baking application; based on the results obtained it could be concluded that the CBWBES can be a very good substitute for conventional clay bake wares both for energy efficiency and good quality of product formation provided that a reduction in the heating up time is achieved in the new ceramic bake ware.

DECLARATION

I, the undersigned, declare that this thesis entitled "*PERFORMANCE ANALYSIS AND REALIABLITY TESTING OF A CERAMIC BAKE WARE (MITAD) FOR AN ELECTRIC INJERA BAKING STOVE*" is my original work done under the supervision of Dr.Ing Demiss Alemu at AAiT during the year 2015 as part of masters of science degree in mechanical engineering (Thermal Engineering stream) and has not been presented for a degree in any University, and that all the source of materials used for the thesis has been duly acknowledged.

Name Signature Date

Garedew Ambaw . _____ _____

(Candidate)

This is to certify that the above declaration made by the candidate is correct to the best of my knowledge.

Dr.Ing:-Demiss Alemu _____ _____

(Thesis Advisor) Signature Date

TABLE OF CONTENTS

SYMBOLS AND ABRIVATIONS

SYMBOLS	NAME	UNIT
A	Area	m^2
V	Average fluid velocity	m/s
L	Characteristic Dimension	m
h_c	Convective heat transfer coefficient	$W/m^2.k$
I	Electrical current	Ampere
ρ	Density	kg/m^2
D	Diffusion coefficient	m^2/s
μ	Dynamic viscosity	$N.s/m^2$
Γ	Element boundary	
ε	Surface Emissivity	
h	Enthalpy	kj/kg
g	Gravitational acceleration	m/s^2
Q_A	Heat generation per unit area	W/m^2
Q	Heat lost or gain	J
ν	kinematic viscosity	$N.s/m^2$
h_{fg}	Latent heat	j/kg
m	Mass	kg
xi	Mass fraction I component	
N	Nusselt number	
p	Resistor power	W
h_r	Radiative heat transfer coefficient	$W/m^2.k$
q	Rate of heat input	W
ε_r	Ratio of vapor diffusion coefficient to total moisture diff.	
N_i	Gallerkin's weighing function	
R_a	Rayleigh number	

LIST OF FIGURES

LIST OF TABLES

CHAPTER ONE

1.1 Introduction

Injera, large pan cake-like bread, is the staple food of Ethiopians. The Injera bake ware (Mitad, in Amharic) is the cultural bake ware used to bake the injera. It is circular in shape and made of clay with size between 45 and 60 cm in diameter. To this end, Mitad is the main energy consuming household item of many Ethiopians. According to the research done by the embassy of Japan, only 10% of the total energy consumption in Ethiopia is supplied by electric power and the rest is from primitive sources, such as wood fuel and dung [1]. The household sector takes nearly 90% of the total energy supply. Access to energy resources and technologies in rural Ethiopia is highly constrained. Physical and economic access to biomass resources is deteriorating because the resources are exploited beyond their carrying capacity. This results in higher household expenditures of labor, time or cash, while modern energy services are still in scarcity. The energy infrastructure is underdeveloped because of the low-economic capacity of the government and other development agents and users [2].

Researches show that rural households use an estimated 50 million m^3 of wood per year for cooking and lighting. This has contributed to rapid loss of tree resources. This in turn has caused loss of soil nutrients and decline in agricultural productivity [3]. In response to these Research done in southern part of Ethiopia reveals that in all settlement typologies, baking injera consumes the most fuel wood and accounts for about 60 percent of total household fuel consumption [2, 20], this being the fact, new development and improvements on this area has been started scientifically in 1983, which most of them are done on enhancing the efficiency of the stove. But, researches conducted to improve the energy efficiency of the clay bake ware (MITAD) were rather rare and ineffective for the intended application.

In the present study the bake ware made from ceramic composites; having a body composition of silica (10%), kaolin (55%), feldspar (10%) and alumina (25%) which was fired to 1220^{o}C and have a thickness of 26mm and diameter of 585mm with built in five turns of 13mm depth spiral groves to embed a resistor wire at the bottom surface of the bake ware. In this study the performance of the new ceramic bake ware was simulated and its reliability for injera baking application was experimentally investigated.

1.2 Statement of the Problem

Given, an efficient insulation system and proper operation of an electric stove, such as the injera baking stove the performance of the overall baking process can greatly be increased. Even though higher efficiency is realizable certain conditions like the cost of materials, the nature the bake ware (having large thermal inertia) and thus the economic status of the customers to afford the price of highly efficient injera baking electric stove is retarding the effort in the energy transition program; from biomass to electricity.

Experimental investigation on the existing clay and ceramic bake ware based stoves revels that, Heating up time required varies according the energy input of the bake ware which was 780 seconds for high power input (3 to 3.5 KW) of conventional electric mitad with 2cm thickness and 60cm dia. and 1080 seconds for low power input (2.2KW) of improved ceramic bake ware (mitad) having 8mm thickness and the same diameter [5]. The study reported an increase in efficiency to 75% from the traditional clay mitad of 52%. Another similar study showed that Given the same thermal property(thermal conductivity, specific heat, and density) and power input, decreasing the thickness of a bake ware results a decrease in heat up time and idle heating time of the bake ware. Given the same thermal property and same bake ware thickness, decreasing power input results an increase in heat up time and idle time [5] and this study reported 71% efficiency in using the new ceramic bake ware based stove.

Although the above researches results in better efficiency of operating the stove; it was also reported that the ceramic bake ware had poor thermal stress resistance and found to produce poor quality of the injera. Poor top porous structure and bottom crust formations on the product were witnessed.

While the thermo physical properties and thermo elastic properties of the materials are the main parameters which affect the efficiency and the strength of the ceramic bake ware; the issue of finding alternatives to improve the efficiency, effectiveness and mechanical strength of the new ceramic bake ware necessitated the need to investigate other ceramic composites for injera baking application.

The aim of this study is to investigate a new ceramic bake ware made from ceramic composites having different thermo physical properties for use in injera baking application.

1.3 Expected Outcomes

The study is expected to pave the way for the development of efficient and reliable injera baking process by providing information on alternative bake ware materials to replace the existing traditional clay bake ware which could significantly reduce the energy efficiency of the traditional way of injera baking process.

1.4 Significance of the Study

In addition to its benefits in providing information on the technical, material and operational requirements of efficient local injera baking electric stove the study is also believed to significantly contribute to the efforts of the country to satisfy the future electric energy needs of the society; by providing adequate information on energy saving opportunities of house hold electric appliances , by providing improved control of household energy bills , also helps to mitigate health problems due to the use of firewood , reduce the rate of deforestation and its accompanying climatic disorder and the risk of wild life migration to the nearby countries.

1.5 Research Objectives

The overall objective of this study was to model the heat transfer during contact baking of injera in a ceramic bake ware based electric stove and to conduct experimental reliability and effectiveness tests of the bake ware for the intended application.

- To determine the effects of physical parameters and material thermo physical properties on the efficiency of the baking process.
- To assess the effectiveness of the ceramic bake ware and identify performance improvement opportunities, optimum alternatives to improve the current electric mitad efficiency and mechanical strength (thermal shock resistance of the ceramic bake ware).
- To compare the performance of ceramic bake ware based baking electric stoves/mitad/ with the conventional clay bake ware stove.
- To develop a numerical heat transfer analysis for an indication of further optimization opportunities.

1.6 Methodology

The methodology followed in this research is based on the objectives formulated above and the full detailed flow chart is as shown in the figure 1.1 below.

Experimental measurement will be conducted to collect data's used to calculate the thermal performance of the electric mitad (baking Disk), the following instruments are used:

- Infrared Thermometer:-to measure the temperature of the bake ware top surface, injera and dough
- Digital mass balance:-to measure the weight of injera and dough.
- Multi-meter:- to measure the input power to the resistant element.
- Measuring tape:-to measure the geometry of the bake wares and heat transfer surfaces.

A finite element method based heat transfer analysis is used to investigate the performance of the stove and to consider further performance optimization opportunities by changing inputs such as thermo physical properties, thickness of the mitad and power source and graphical plot of the result at different working conditions were developed as output.

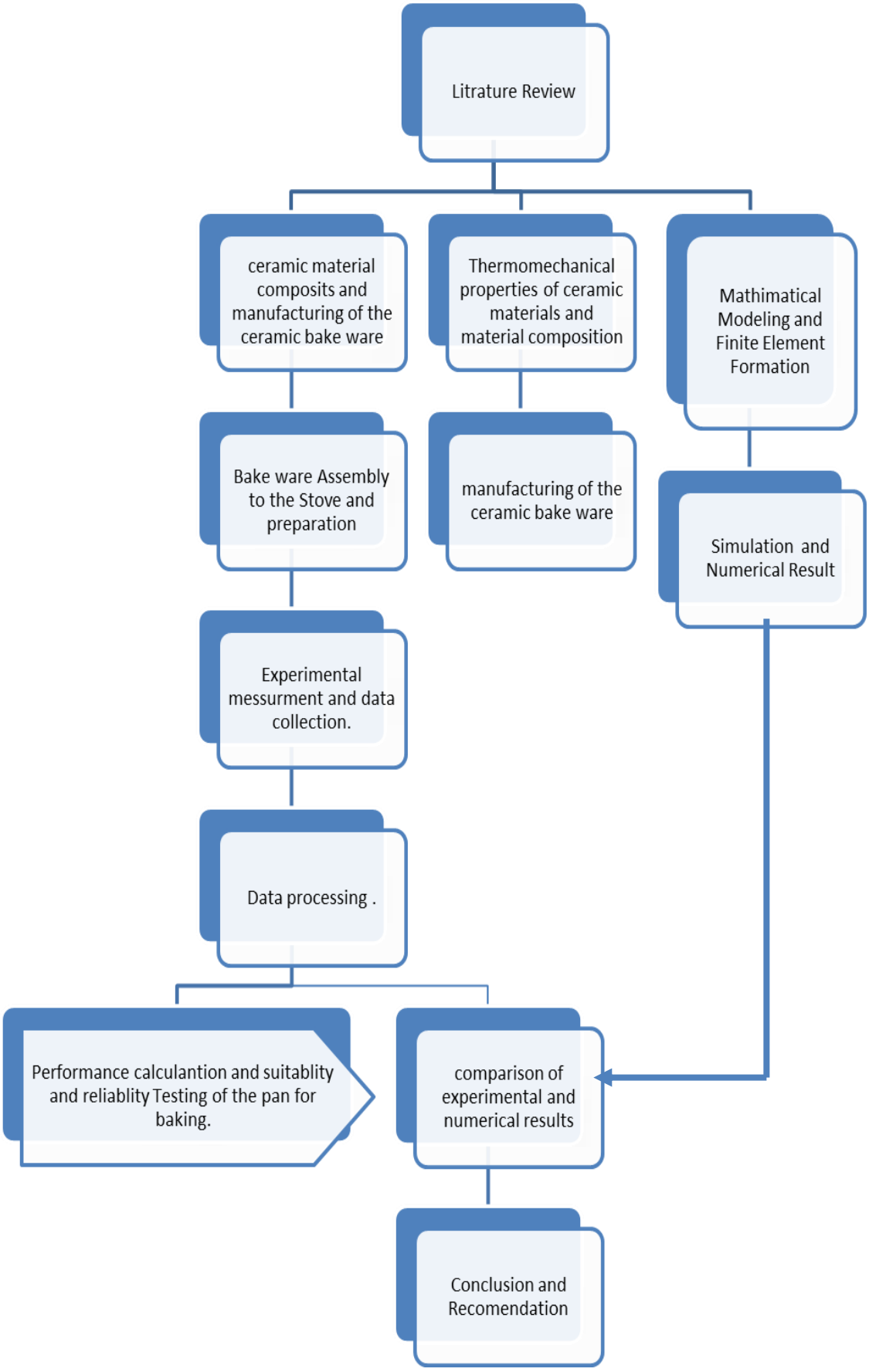

Figure 1-1: *Flow chart of the present work.*

CHAPTER TWO

LITRATURE REVIEW

A substantial number of studies have been reported in the literature on food processing (drying, Baking, frying .etc.). Some of them are reviewed in this section. The literature review part of this Thesis consists of two sections. The first section is a review of injera making process, thermo-physical properties of food stuffs and their determination and on thermal stress characteristics of ceramic bake ware. The second section reviews the heat transfer theories, models, and the relevant numerical techniques used in food processing.

2.1 Injera Baking Process

In making injera,teff flour is mixed with water and allowed to ferment for three to four days, as with sourdough starter.as a result of this process, injera has a mildly taste. The injera is then ready to bake in to large flat pan cake bread. This is done either on a specialized electric stove or, more commonly on a clay plate (Mitad) placed over a fire. Unusual for yeast or sourdough bread, the dough has sufficient liquidity to be poured on to the baking surface, rather than rolled out. In terms of shape, injera compares to the French crepe and the Indian dosa as flat bread cooked in a circle and used as a base for other foods. The bottom surface of injera, which touches the heating surface, will have a relatively smooth texture, while the top will become porous. This porous structure allows the injera to be a good bread to scoop up sauces, dishes and doro wet. Figure 2.1 shows injera and the bake ware or mitad.

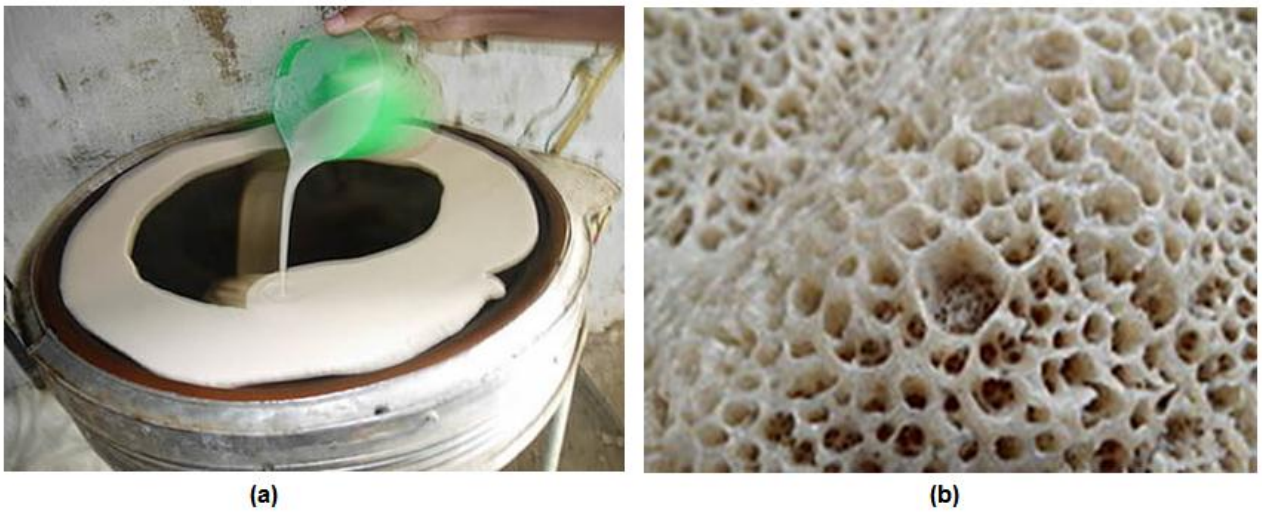

Figure 2-1: *The injera baking process: (a) poring of the dough over hot bake ware called Mitad in Amharic (b) the top surface texture of the final product, injera.*

2.1 Energy Sources for Injera Baking

The two energy sources mainly used for injera baking processes are Biomass and Electricity; the biomass fuel (mainly dry wood) is used in open fire system, in this case the heat energy due to the burning of the dry woods is convicted to the mitad bottom surface in a suitably designed stove. But the energy source from electricity is produced by a heating element situated at the bottom surface of the mitad; the heat produced in the heating element is directly conducted to the mitad by conduction.

2.1.1 The bake ware (Mitad)

The mitad is a round circular disk with a smooth top surface suitable for injera baking application, the traditional mitad is made of clay materials having low thermal conductivity and thermal diffusivity, which makes it suitable for slow cooking (browning) application; however the energy efficiency of the mitad made of clay is very poor, around 52 to 55 % as reported by different researches conducted on the area [4, 5].

Generally two ways of energy supply are mainly adopted in Ethiopia, one is biomass, which accounts more than 85% and the other is electricity; mainly used in urban cities.

This thesis was based on electricity as a source of energy. The electric line is bought from the Ethiopian electric power corporation (EEPCO) and consumers are charged monthly consumption fee.

2.1.2 Resistance Heating System

Resistance heating involves passing line frequency current through high resistance heating elements. The resistance to the current flow generates heat in the Ni-Cr coil (Figure 2.1); and the heat is transferred to the process or material via conduction. Ni-Cr or Nicrome is a non-magnetic alloy that is commonly made up of 80% nickel and 20% chromium, it has a resistivity ranging from 1.1 to 1.5 $*10e^{-6}\Omega m$ and a very high boiling point ($1400^{o}C$), such a low electrical resistivity and high boiling point makes Nicrome a very good conductor of electricity and idle material for making wires, heating elements and other insulation devices [5].

Nicrome is commonly wound up in to coils and used in heating elements (devices that convert heat in to electricity through joules heating as in air dryers, toasters and ovens).this is given in figure 2.2 bellow.

Figure 2-2: *Closed coil Nicrome heating element (Nicrome 80 and other resistance alloys, technical properties data, wirtron.com).*

In general, mathematical power dissipated in an electric resistance wire can be expressed as [5].

$$P = \frac{V^2}{R} \tag{2.1}$$

Where: - P is the power dissipation, V is the line voltage and R is the resistance of the wire.

$$R = \frac{\gamma L}{A} \tag{2.2}$$

$$\gamma = \gamma_o\left(1+\alpha_T(\Delta T)\right) \tag{2.3}$$

Where : γ is the resistivity of Nicrome wire (ranging from 1×10^{-6} to $1.5\times10^{-6}\Omega$m at 20 ^{o}c), L is the length of the wire, and A is the area of the wire (m^2), γ_o is cold resistivity of the wire at room temperature and α_T is the thermal expansion coefficient (0.000014/K) [5].

The power dissipated in a resistance heater depends on the current flowing through it. In Ethiopia the line voltage in a house hold varies between (220 to 250 AC). In equation 2.1, for a maintained potential or line voltage, the power dissipated in the heater depends on the magnitude of the resistance. Nicrome wire has a positive temperature coefficient, meaning its resistance to current flow increases as the temperature of the wire increases as given by Eqn. (2.3) [5] this is easily seen by substituting equation 2.2 in 2.3. And assuming constant length of the wire before and after heating, the resistance of the heater increases as it gets hot and hence the reduction of the power dissipation from the value at room temperature. Equation 2.4 describes the relationship between the hot and cold resistance of the wire.

$$R_h = R_c\left(1 + \alpha_T(\Delta T)\right) \tag{2.4}$$

2.2 Cooking Methods and Materials

Cooking methods can be characterized into two main types: dry heat cooking and moist heat cooking. Dry heat cooking heats foods in the absence of water, and includes methods such as baking and roasting, and bake ware-frying. Moist heat cooking uses water to heat food, and include boiling, simmering, braising, and steaming [8, 9, and 12].

Ovens are used in many dry heat methods. Electric ovens use two heating coils, located at the top and bottom of the oven. The bottom coil is used for baking and roasting; the top is used for broiling. The heating coils are simply resistive elements which are heated by passing an electric current through them. Cooking in oven and stove tops are the main dry heat cooking methods, cooking on the stovetop utilizes conduction through a bake ware to heat the contents. In dry heat cooking, heat is conducted directly from the bake ware to the food, as shown in Figure 2.3. The heat is generated by resistive elements on electric stovetops. And Heat transfer inside an oven is actually more complicated than simply conduction and convection. The heating element emits a considerable amount of radiation which also contributes to the heating of the food. For the purpose of the present study only cooking on stove top is reviewed [8, 9, and 12].

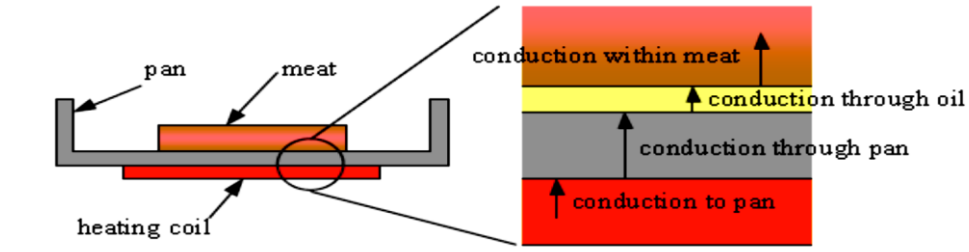

Figure 2-3: *A typical cooking arrangement on stove tops (Commercial Cooking Marking and Application Guide, UL and the UL logo are trademarks of UL LLC © 2012)*

Moist heat methods use water in various states to heat food. The most common state is boiling, where water is heated by conduction through a pot on stovetop, and the heat is transferred to the food through convection. Deep frying and microwave are also cooking methods [8, 9].

Injera baking can be categorized as a contact baking method where the dough is poured on the surface of a hot bake ware, the bake ware or mitad may acquire the heat either from open fire burning of biomass fuels or from an electric heater embedded at one side of the mitad, in the latter case the heat conducted from the heater to the bake ware is directly supplied to the

dough and this heat is used to evaporate the moisture from the dough and to raise the temperature of the product to the boiling temperature of water. The contact baking process is explained and modeled in detail in chapter 3.

2.2.1 Cooking Materials

Most cooking containers are metals or ceramics, due to their ability to withstand high temperatures. Common metals are aluminum, copper, tin, stainless steel, and cast iron. Ceramics include glass, porcelain, earthenware, and stoneware. In addition, non-stick coatings and enamel coatings may be used on the surfaces to improve the properties [8, 9].

Thermal conductivity, density, and specific heat are three very important factors in determining what cooking material is best suited for the kitchen. A high conductivity material tends to have a more even temperature distribution than one with a low thermal conductivity. A material with low specific heat requires less thermal energy to heat; therefore, it heats faster than one with a high specific heat [8, 9, and 12]. Thermal diffusivity (α) is the combination of the three properties:

$$\alpha = \frac{k}{\rho C_P} \tag{2.5}$$

Where k is the thermal conductivity, ρ is the density, and c_p is the specific heat. Thermal diffusivity measures the effectiveness by which a material conducts thermal energy with respect to its ability to store thermal energy. A material with high α is characterized by a quick response to the changes in surrounding temperatures. A material with low α takes longer to reach a steady state condition, but is excellent at retaining heat once heated (ceramics and clay) [8, 9, and 12]. So enhancing the cooking or baking efficiency of a bake ware requires optimizing the thermal diffusivity of the material while keeping the density and heat capacity fixed or the other way round; in doing this the cooking rate required should not be compromised.

2.2.2 Ceramic as a Cook Ware

Ceramic is usually a compound of metallic and non-metallic elements. They are poor conductors of heat, but are excellent at retaining heat once heated. They are very resistant to corrosion and are non-toxic. Due to their ability to retain heat, dishes made of thick ceramic materials will keep foods warm longer than metallic serving dishes of comparable shape and size.

A common problem with most ceramics is their tendency to crack due to thermal stress. Since they are such poor conductors of heat, there may be a large temperature difference between one side of the bake ware and the other. In such case, the warmer side expands more than the other, causing the bake ware to crack. Ceramic bake wares are seldom used on stovetops for this reason; ovens allow even heating from all sides, preventing large thermal gradients [8, 9].

2.2.3 Thermo Mechanical Behavior of Ceramic Bake Wares

The susceptibility of ceramic materials to thermal stresses has been recognized for a long time. The first quantitative treatment of thermal stress fracture in ceramic materials was prepared by Winkelrnann and Schott (1894). Then after; Hofstadter and Everhart (1902) gave a correct solution for the case of infinitely rapid cooling slab. A number of investigators considered testing methods for glasses and for refractories and their correlation with service results. Norton (1926) studied the problem and first suggested that shear stresses must be considered as well as tensile stresses. More recently, several investigators, particularly those interested in special refractory applications, have considered the problem of thermal stresses from both theoretical and experimental points of view. New attempts have been made to define and to measure a material property which can be called "resistance to thermal stresses." Although these attempts have not been completely successful in a quantitative way, they have led to a much improved understanding of the factors that contribute to thermal stress resistance. The purpose of the present paper is to experimentally investigate the reliability and the effectiveness of the selected ceramic bake ware for injera baking application.

2.3 Origin and Analysis of Thermal Stress

The origin of thermal stresses is the difference in thermal expansion of various parts of a body under conditions such that free expansion of each small unit of volume cannot take Place. This condition can arise in a number of ways:

2.3.1 Stress Arising at Uniform Temperature

If a ceramic body is changed from an initial temperature, t_o, to a new uniform temperature, t', no stresses arise providing that the body is homogeneous, isotropic, and unrestrained (free to expand). Under these conditions, the linear expansion of each volume element is $\alpha (t' - t_o)$ and the shape of the body is unchanged [12, 21].

If the body is not homogeneous and isotropic, as in a mixture of two materials (such as a glass-mullite and porcelain) stresses will arise due to the difference in expansion between crystals or phases. The magnitude of the stresses will depend on the elastic properties and expansion coefficients of the components. Similarly, if a bar of material is completely restrained from expansion by the application of restraining forces due to the design of a part, stresses arise due to the restraining boundary, so this additional stress must be added to get the total stress experienced by the structure [21].

For free expansion or contraction in a homogeneous and isotropic solids that is heated or cooled uniformly, that is if no temperature gradients are imposed the solid will be stress free, if however the motion of the body is restrained by rigid end supports thermal stresses will be induced the magnitude of the stress σ resulting from a temperature change from T_o to T_f as given by (Hasselman 1963, 1969; Kingery et al. 1976, 816) is:

$$\sigma = E\alpha_l(T_f - T_o)S = SE\alpha_l\Delta T \tag{2.6}$$

The shape factor varies for different shapes. It is assumed that the bake ware is a thin disk and the shape factor is derived from this assumption, for a thin disk *S* is 1/ (1-2μ) as given by (Hasselman 1963, 1969; Kingery et al. 1976, 816).

And the critical temperature difference for fracture is given by substituting σ Withσ_f, Where σ_f is the magnitude of stress at fracture.

$$\Delta T_{fracture} = \frac{\sigma_f}{E\alpha_l} S \tag{2.7}$$

Where E is the modulus of elasticity and α_l is the linear coefficient of thermal expansion. Upon heating ($T_f > T_0$), the stress is compressive ($\sigma < 0$), during cooling a tensile stress will be imposed.$\Delta T_{fracture}$ It is the critical temperature difference to fracture and S is the shape factor of the body. Equation 2.7 is only applicable for high rates of heat transfer, at low rates of heat transfer equation 2.7 is multiplied by thermal conductivity [W. d. kingery, 21]. Typical thermo mechanical properties of a ceramic body are as tabulated bellow taken from [17].

Table 2-1: *Initial guess values of parameters (Cold science and marine technology, thermo mechanical properties of materials-Aleksey V.Marchenko)*

$\sigma_{tension}$ (MPa)	E (Gpa)	K (w/m.c)	μ	Cp (kj/kg.k)	β ($1/c^o$)	ρ(kg/m^3)
54.045	0.296	0.9-2	0.2	960	$2.2*10^{-6}$	2400

In this paper analytical solution of the stress developed in the body were calculated from a simulated temperature distribution both during heat up and baking stages, the temperature difference which can cause fracture in the body were also calculated, the cyclic stress variation is simulated in chapter 4.

2.3.2 Stress Arising Due to Temperature Gradient

When a solid body is heated or cooled, the internal temperature distribution will depend on its size and shape, the thermal conductivity of the material, and the rate of temperature change. Thermal stresses may be established as a result of temperature gradients across a body, which are frequently caused by rapid heating or cooling, in that the outside changes temperature more rapidly than the interior; differential dimensional changes serve to restrain the free expansion or contraction of adjacent volume elements within the piece. For example, upon heating the surface, the exterior of a specimen is hotter and, therefore, will have expanded more than the interior regions. Hence, compressive surface stresses are induced and are balanced by tensile interior stresses. The interior–exterior stress conditions are reversed for rapid cooling such that the surface is put into a state of tension [12, 17, and 21].

2.3.3 Thermal Shock of Brittle Materials

For ductile metals and polymers, alleviation of thermally induced stresses may be accomplished by plastic deformation. However, the non -ductility of most ceramics enhances the possibility of brittle fracture from these stresses. Rapid cooling of a brittle body is more likely to inflict such thermal shock than heating, since the induced surface stresses are tensile [12] as sown in the figure bellow. Crack formation and propagation from surface flaws are more probable when an imposed stress is tensile [21].

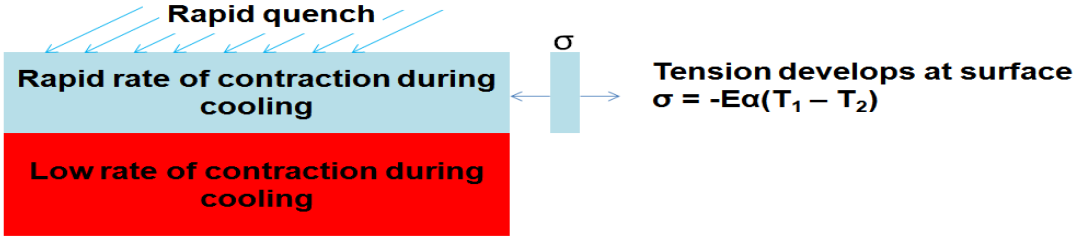

Figure 2-4: *Illustration of the development of tensile stress on the top surface of a rapidly quenched tin layer (P. Vincenzini (ed.), Fundamentals Of Ceramic Engineering, Elsevier Science Publishers, Ltd.,New York, 1991.)*

The capacity of a material to withstand this kind of failure is termed its thermal shock resistance. For a ceramic body that is rapidly cooled, the resistance to thermal shock depends not only on the magnitude of the temperature change, but also on the mechanical and thermal properties of the material. The thermal shock resistance is best for ceramics that have high fracture strengths σ_f and high thermal conductivities, as well as low moduli of elasticity and low coefficients of thermal expansion. The resistance of many materials to this type of failure may be approximated by a thermal shock resistance parameter TSR or R:

Thermal shock occurs when a substrate is exposed to temperature extremes in a short period of time, under this condition the substrate is not in thermal equilibrium and internal stresses may be sufficient to cause fracture [17].

The thermal shock resistance of pottery vessels provides a measure of their ability to survive rapid changes in temperature without fracture. As with strength and toughness, in order to understand and assess thermal shock resistance one needs to consider, first, the initiation of cracks and, second, the propagation of these cracks to the ultimate failure of the vessel (Hasselman 1963, 1969; Kingery et al. 1976, 816).

The primary driving force for crack initiation in thermal shock is the stresses due to the differential expansion or contraction of the inner and outer surfaces of a pottery vessel resulting from a rapid change in temperature at one surface, and thus temperature gradients through the vessel wall. Assuming that there is insufficient time for heat conduction between the two surfaces, the stress (σ) that results from a temperature difference (ΔT) is given by:

$$\sigma = \frac{SE\alpha_l \Delta T}{(1-\mu)} \tag{2.8}$$

Where E is Young's modulus, α is the linear thermal expansion coefficient, μ is the Poisson ratio and S is a geometrical constant determined by the shape of the vessel. Hence, crack initiation occurs when the temperature difference (ΔT_c) between the two surfaces is sufficiently high that the resulting stress is equal to the fracture strength (σ_f) of the ceramic; that is,

$$\Delta T_C \cong \frac{\sigma_f (1-\mu)}{SE\alpha_l} \tag{2.9}$$

$$\alpha_l = \frac{\Delta L}{\Delta T L} \tag{2.10}$$

2.3.4 Assumption of the thermal Stress Development in the Ceramic mitad

For the present study the ceramic body was assumed to be isotropic and there is no restriction of the body from free expansion by rigid thermal boundaries; so the stresses due to temperature gradient and sudden cooling will be investigated. Based on the data's given in table 2.2, the maximum temperature change for fracture can be estimated as. For medium heat transfer rates equation 2.9 was modified as.

$$TSR \cong \frac{k\sigma_f * (1-\mu)}{SE\alpha_{\ l}} = S * 84.32 kj/ms \tag{2.11}$$

Substituting the shape factor the TSR value becomes:

$$TSR = 84.32 * \frac{1}{(1-2*0.2)} = 140 Kj/ms \tag{2.12}$$

Or considering high heat transfer rate and using equation 2.9 gives the maximum allowable temperature change for fracture as:

$$\Delta T_c = \frac{140 kj/ms}{1.27} = 110.656\,°C \tag{2.13}$$

Temperature changes beyond this may cause the material to crack; and eventually to separate to pieces. The sensitivity of a ceramic materials to thermal shock may be also determined by experimental method(hasselmann 1993,et.el),In this method a specimen (flexural test specimen) is heated to a specified temperature and then quenched , the specimen cools rapidly by a change in temperature of magnitude the difference between the temperature before and after quenching the specimen, after quenching the flexural strength of the specimen is measured by standard flexural bending test, and subsequent results are plotted for strength verses change in temperature. When the change in temperature reaches a certain

value the specimen strength falls sharply, this change in Temperature is a parameter indicating the TSR of the material.

In this study only numbers of cycles of heating and cooling tests are conducted; the bending tests are not performed due to difficulties in obtaining test specimen from tabor ceramic Plc.

2.3.5 Prerequisite for the use of the ceramic bake ware for baking application

The characteristics of ceramic bake ware for food cooking or baking application should include the following features.

- The ceramic material should withstand sudden changes in temperature (relatively higher thermal shock resistance is required), since the process of injera baking requires heating of the baking disk or bake ware to the baking temperature, usually from 180 to 200^{o}C and a sudden cooling of the disk with the dough, which is around 25^{o}C.
- The ceramic bake ware should have the ability to withstand moderate mechanical loads applied to clean the surface of the bake ware from residual baking residuals
- The ceramic bake ware should have a non-stick top surface for the quality of the injera baked; i.e. the baking disc should be effective during baking cycles.
- The ceramic bake ware should provide efficient cooking condition.
- The ceramic material should withstand stress due to temperature gradient across the thickness.
- The ceramic material used should be free of health problems.

To improve the TSR (thermal shock resistance) of a ceramic material we can change the compositions to provide a ceramic matrix with low thermal expansion coefficient, high thermal conductivity or low modules of elasticity and high strength, this is clearly seen from Equation 2.8.

2.3.6 Selection of Ceramic Composite for Baking Application

The ceramic body that should be used for injera baking application should be composed of material composites which fulfill the operational requirements; previous researches on similar

area used a ceramic bake ware and the result sowed that the bake ware was unable to withstand the intended application; failure due to crack and poor quality of injera was observed.

A research conducted in sirilanka(P.P.S.S. Pussepitiya and S.U. Adikary), Optimum thermal shock resistance of 0.74 kJm-1s-1 was achieved for a body composition of 45% of clay, 15% of talc, 15% of alumina and 25% of zirconium silicate which was fired to 1250^0C [17]. Further, modulus of rupture and coefficient of thermal expansion of the ceramic body were 74 MPa and 30.2×10-7 K-1, respectively. These results suggest that the ceramic body is suitable to be used in cookware applications. This research is based on a newly manufactured ceramic body with a body composition of silica (10%), kaolin (55%), feldspar (10%) and alumina (25%) which was fired to 1220^oC with a thickness of 26mm and diameter of 585mm with built in five turns of 13mm depth spiral groves to embed a resistor wire at the bottom surface of the bake ware body.

2.3.7 Manufacturing Steps of the Ceramic Body

Figure 2.5 shows the process flow diagram of the ceramic cookware. The slip casting method is capable of producing uniform thickness of ceramic article. The product is fabricated with slip casting.

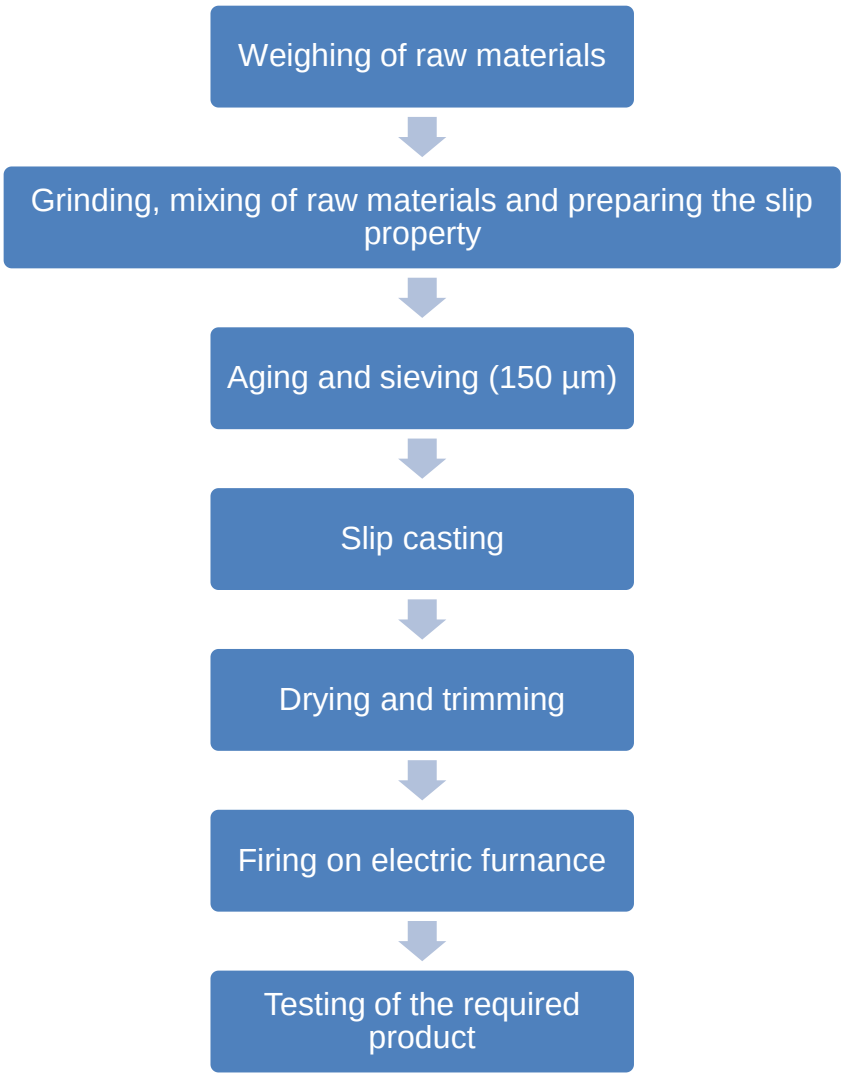

Figure 2-5: *Manufacturing steps of ceramic bake ware (Dinsdale, A., Pottery science, Materials, Processes and Products, first edition, John Wiley & sons, 1986, p.94 and p.112.)*

2.4 Cooking and Heat Transfer

Heat transfer during cooking or baking with the use of a vessel or bake ware is based mainly on two processes of heat transfer, *conduction* and *convection* mode of heat transfer. Conduction is the transfer of heat in solids or nonmoving fluids due to interaction between the molecules or atoms of the material and convection involves the transfer of heat between a solid and moving fluid with a differential temperature, a further heat transfer process is radiation, which usually be neglected since the temperature achieved during cooking are still comparably moderate. While different heat transfer processes come in to play between the vessel or bake ware and food stuff, heat transfer within a vessel is determined by heat conduction as described by (kingery et.al.1976) is:

$$\frac{dQ}{dt} = -k.A.\frac{dT}{dx} \tag{2.14}$$

Where -$\frac{dT}{dx}$-is the temperature gradient. $\frac{dQ}{dt}$ Is the heat flow through the area A and $k$is the thermal conductivity of the vessel material. If temperature is not steady, the temperature development is described by Eqn. (2.14)

$$\frac{dT}{dt} = \alpha.\frac{d^2T}{dx^2} \tag{2.15}$$

Heat transfer within a vessel is thus directed by its material properties, in particular thermal conductivity but also heat capacity and density, and that is why these material properties are of importance for ceramic vessel or bake ware expose to heat.

Superior thermal conductivity results in an even heat distribution, and a bake ware made of a material with good thermal diffusivity (accordingly thermal conductivity) shows rapid response to changes in temperature.

In a material with low thermal conductivity, uneven heating creates hot spots, where foods can easily be burnt. Materials in which the thermal conductivity and the thermal diffusivity are low and heat capacity relatively high take longer to reach a steady state conduction but they are excellent at retaining heat once their contents are heated up. It is for these specific thermal properties that today, ceramic vessels are commonly used for slow cooking of foods and simmering of stews or casserole, while materials with higher thermal conductivity are normally chosen to boil or fry food stuff(Hein el,al. 1990).

The second heat transfer process which has to be considered during cooking is the heat convection, heat convection emerges between the bake ware top surface and the food stuff, such as injera, between also the ambient air and outer surface of bake ware, and this can be described by

$$\frac{dQ}{dt} = -h.A.(T_s - T_\infty) \tag{2.16}$$

Where h is the convective heat transfer coefficient, A is the area of the surface of the fluid.T_s is the surface temperature and T_∞ is bulk temperature of fluid.

In contrast to heat conduction heat convection is not affected by the properties of the vessel material, in terms of technical choice convection can only be controlled through shape parameters, thus affecting the contact area of interface between the ceramic vessel and the

moving fluid. Also important to the cooking process is the heating efficiency η (Hein el,al. 1990) the ratio between the energy Ecook consumed in actual cooking process and the energy Qheat inserted in the system.

$$\eta = \frac{E_{cook}}{Q_{heat}} \tag{2.17}$$

The higher the efficiency is, the faster will be the food stuff be heated during the baking or hating phase and the less fuel is required to maintain temperature once it is reached. Earlier studies have investigated heat transfer through examining what was termed heating or cooking effectiveness (Skibo, et.al.1989, Schiffer 1990, Pierce 2005). While these studies mainly attempted to assess the influence of *surface treatment*, i.e. *vessel shape* and *permeability*, or *heating rates*, the *thermal conductivity* of a material plays a significant role in heating efficiency of a ceramic and greatly influence the time required to heat up food (Hein.et.al, 1990).

Heat transfer by radiation requires no materials medium. It is accomplished by means of wave motion through space. All objects can emit and absorb radiation, and radiation carries energy. When an object emits radiation, it gives of energy, and when it absorbs radiation, it takes in energy. Sometimes, the emission or absorption will take place only in certain parts of the spectrum and sometimes they are distributed all across the spectrum. The amount of radiation emitted by an object is given by:

$$Q_{emitted} = \varepsilon\sigma . AT^4 \tag{2.18}$$

Where Q_{mitted} is the heat flux energy per unit time, *A* is area of heat flux intensity, σ is the Stefan Boltzmann constant (5.67 x 10^{-8}) 10/m2 (K4), ε is a material property called emissivity and *T* is the absolute Temperature. The emissivity has a value between zero and 1, it measures the efficiency of a surface to emit heat by radiation. The amount of heat absorbed by a surface is given by:

$$Q_{absorbed} = \alpha . I \tag{2.19}$$

Where *I* is the incident radiation determined by the amount of radiation emitted by the object and how much of the emitted radiation actually strikes the surface. The latter is given by the *shape factor, F,* which is the percentage of the emitted radiation reaching the surface. The net amount of radiation absorbed by the surface is:

$$\mathrm{Q_{absorbed}} = \mathrm{F}.\alpha_2\varepsilon_1\sigma.\mathrm{AT}^4 \tag{2.20}$$

For an object in an enclosure, the Radiative exchange between the object and the wall is greatly simplified as given by Eqn. (2.22). This simplification is realistic because all of the radiation emitted by the object strikes the wall ($FO_{bject----wall} = 1$).

$$Q_{enclosure} = -\sigma \varepsilon_{object} A_{object} \left(T_{object}^4 - T_{wall}^4\right) \quad (2.21)$$

The three phenomena of heat transfer may take place one at a time or may occur simultaneously in a given system.

2.5 Thermo-physical properties

The thermo physical properties of foods are required in order to calculate process times and to design equipment for the storage and preservation of food. There are a multitude of food items available, whose properties are strongly dependent upon chemical composition and temperature. Composition-based thermo physical property models provide a means of estimating properties of foods as functions of temperature. Constituents commonly found in food items include water, protein, fat, carbohydrate, fiber, and ash. Choi and Okos (1986) have developed equations presented in APPENDEX D to E for predicting the thermal properties of these components and ice as functions of temperature in the range of −40°C to 150°C.

Choi and Okos (1986) reported that the equations presented in Appendix D to E produce an error of 6% or less and these equations are used in the present study; the percentage composition of the major components of fermented cereals is given in the FAO report. The percentage composition of teff injera as taken from the FAO report is shown in Figure 2-6.

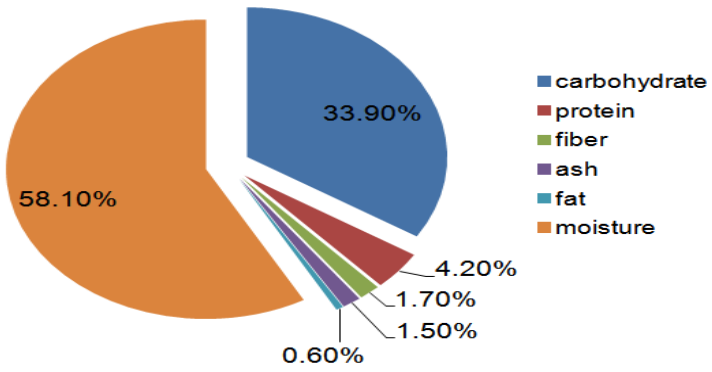

Figure 2-6: *Composition of teff injera in percentage by weight. Taken from the FAO report (food composition data production management and use, food and agriculture organization of the united nation 2003)*

For the present study the mass and volume fraction of the injera compositions were taken from previse literatures on the area [4, 6] this are tabulated in Appendix D to J.

2.5.1 Specific Heat Capacity

The specific heat of food stuff is defined as the quantity of thermal energy associated with a unit mass of the food and a unit of change in temperature. This thermo-physical property is often referred to as heat capacity and is an essential component of a thermal energy analysis on a food product, a thermal process, or processing equipment used for heating or cooling of a food. Specific heat capacity depends on the nature of the heat addition process in terms of either at constant pressure or at constant volume. However, since pressure change in heat transfer problems of food materials are usually very small, the specific heat at constant pressure is most often considered [7,28].

$$c_p = \frac{Q}{m\Delta T} \tag{2.22}$$

Where *Cp* is the specific heat (*J/kg.K*), *Q* is the heat loss or gained (*J*), *ΔT* is the temperature change (*K)*, and *m* is the mass of the food (*kg)*

The specific heat is sensitive to the composition of the materials if the specific heats of individual components are different; and to the interactions between the components of the material. Choi and Okos (1986) proposed use of the following composition based equation together with empirical equations predicting the specific heat of each pure component as a function of temperature there by including both composition and temperature dependence in the specific heat estimate of the mixture this is tabulated in appendix E.

$$c_{pmixture}(T) = \sum_{j=1}^{n} c_{pi}(T) w_i \tag{2.23}$$

Where: - c_{pi} is the specific heat of the individual food component and x_i is the mass fraction of the food components. The specific heat is a function of temperature for every component is tabulated in appendix D and E.

2.5.2 Thermal conductivity

Thermal conductivity relates the conduction heat transfer rate to the temperature gradient. A food's thermal conductivity depends on factors such as composition, structure, and temperature of the food item.

Early work in the modeling of the thermal conductivity of foods includes Eucken's adaption of Maxwell's equation (Eucken 1940). This model is based upon the thermal conductivity of dilute dispersions of small spheres in a continuous phase [28]:

$$k = k_c \frac{1 - [1 - a(k_d/k_c)]b}{1 + (a - 1)b} \tag{2.24}$$

Where k is the conductivity of mixture, k_c is the conductivity of continuous phase; k_d is the conductivity of dispersed phase

$$a = 3k_c/(2k_c + k_d) \tag{2.25}$$

$$b = V_d/(V_c + V_d) \tag{2.26}$$

Where V_d is the volume of dispersed phase and Vc is the volume of continuous phase.

For multi-component systems, numerous researchers have proposed the use of parallel and series thermal conductivity models based upon the analogy with electrical resistance (Murakami and Okos 1989). The parallel model is simply the sum of the thermal conductivities of the food constituents multiplied by their volume fractions:

$$k = \sum x_i^v k_i \tag{2.27}$$

Where: - x_i^v is the volume fraction of constituent *i*. The volume fraction of constituent *i* can be found from the following equation:

$$x_i^v = \frac{x_i/\rho_i}{\sum(x_i/\rho_i)} \tag{2.28}$$

The perpendicular model is the reciprocal of the sum of the volume fractions divided by their thermal conductivities:

$$k = \frac{1}{\sum x_i^v k_i} \tag{2.29}$$

These two models have been found to predict the upper and lower bounds of the thermal conductivity of most foods. Saravacos and Kostaropoulos (1995) suggest that the parallel structural model can be used to calculate the thermal conductivity of porous food items including granular, puffed, or freeze-dried foods, while the series model can be used to calculate the thermal conductivity of low-porosity food items, including gelatinized starchy foods or high-sugar foods. The mass fraction of the constituents and determination of the thermal conductivity of injera are as tabulated in appendix I and J.

2.5.3 Density

Density is the ratio of mass to volume of a material. Density of food products is an important Property in analyzing food processing operations. Density is closely related to porosity and moisture content of food. The structure of food materials can be characterized by density (apparent and true), porosity, specific volume, particle density shrinkage and so on. Among these, density and porosity are the most common structural properties.

Apparent density:-the density measured in order to include the volume of the solid and liquid material, and all pores closed or open to the surrounding atmosphere.

$$\rho_{ap} = \frac{m_t}{v_t} \tag{2.30}$$

Where m_t is the total mass and v_t is the total volume including the pores.

Substance density or (True density):-the density measured when the substance has been brocken,milled,or masshed to guarantee that no pores remain.

$$\rho_T = \frac{m_t}{v_p} \tag{2.31}$$

Where, $Vp = Vs + Vw$, is the total volume of the sample excluding pores (volume of dry solids and water).Density is an intensive property it depends directly on the mass fractions of the major components of the food and can be found from:

$$\rho = \frac{1}{\sum_{i=1}^{n} x_i / \rho_i} \tag{2.32}$$

Where ρ is the density of the product $kg/m3$, ρ_i is density of each food component and x_i is the mass or weight fraction of each food component. An empirical relation for the determination of density of major food components as a function of temperature is given in Table 1-2 [Appendix D and E].

2.5.4 Thermal Diffusivity

Thermal diffusivity indicates how fast heat propagates through a sample while heating or cooling. Thermal diffusivity is a parameter used in the heat transfer calculation by conduction. The rate at which heat diffuses by conduction through a material depends on the thermal diffusivity and can be defined as:

$$\alpha = \frac{k}{\rho cp} \tag{2.33}$$

Where α is thermal diffusivity (*m2_/*s), ρ is density (*kg/m*_3), Cp is specific heat capacity (*J/kg.K*_), and k is thermal conductivity (*W/m.K*). Thermal diffusivity can be determined either by direct experiment or estimated from the thermal Conductivity, specific heat, and density data.

2.5.5 Moisture Diffusivity

Moisture diffusivity, D is the rate at which moisture diffuses through a material. Moisture Diffusivity is an important transport property necessary for the design and optimization of all the Processes that involve internal moisture movement. Fick's second law is used in liquid diffusion Theory to establish moisture diffusion as a function of the concentration gradient as given for cylindrical two dimensional domains is:

$$\frac{\partial w}{\partial t} = \frac{1}{r}\left(\frac{\partial}{\partial r}\left(Dr\frac{\partial w}{\partial r}\right)\right) + \frac{\partial}{\partial z}\left(D\frac{\partial w}{\partial z}\right) \tag{2.34}$$

Where W is concentration (kg/m^3), *D* is diffusion coefficient (m^2/s), x is material thickness along direction of mass transfer (m), and t *is* time in(s).

2.6 Contact Baking Process and Heat Transfer Theories

2.6.1 Contact Baking Process

Contact baking is a widely applied process used in food processing applications for example baking of crisp bread, tortillas, pizzas, chapatti, pan cakes, pita breads etc. Being a traditional process, optimization and process control to obtain the desired final product quality is still largely based on experience and good craftsmanship rather than on predictive, engineering calculations [16]. A transition from this traditional empirical approach towards methods that rely on calculations based on predictive models requires a deeper mechanistic understanding of the contact baking process and a knowledge of the physics involved, particularly heat and mass transfer [16]. During the baking process heat and mass transfer occur simultaneously and induce many complex physical–chemical processes such as evaporation of water, crust formation, browning reactions, denaturation of proteins, and gelatinization of starch, (Lee et al., 1996; Mondaland Datta, 2008; Sablani et al., 1998; Therdthai and Zhou, 2003). In the literature, there are only a few publications on the modeling of contact baking (Gupta, 2001; Pyle, 2005) and the related contact frying process (Bake ware et al., 2000; Bake ware and

Singh, 2002; Wichchukitet al., 2001), as compared to baking in a convection oven. Pyle (2005) studied the baking of crumpet (a product made of diluted batter). Pyle (2005) did not obtain a good agreement between the measured and the simulated temperature profile.

2.6.2 Heat Transfer Models in Food Processing

The heat and mass transfer play an important role in baking (Mondal and Datta, 2008, Sumnuand Sahin, 2008), frying (Skjöldebrand and Hallstroem, 1980) and drying (Srikiatden and Roberts, 2007). There is a strong coupling between temperature and moisture content. When a solid food is heated, the water inside the food migrates either in the form of liquid water or in the form of liquid water and water vapor (Thorvaldsson and Janestad, 1999). The temperature and water content inside a solid food are varying in space and time during a heat treatment. Their entire history and their spatial distribution influence the quality and the safety of the processed foods. For example the acrylamide formation during bread baking (Ahrne et al., 2007) and production of the breakfast cereal (Jensen et al., 2008) depend upon the temperature and the heating time. Further, a quantitative understanding of heat and mass transfer in food process is also an essential role for scale up to industry. Generally, there is a great need for a quantitative understanding of heat and mass transfer to optimize and control the final product quality. Developing mathematical models of solid food processes such as baking and frying require physical as well as mathematical insight into a food material and the processes (Halder, et al., 2011).

The analysis of heat and mass transfer in a food system is very important because food properties change with temperature and moisture movement during the process. A mathematical model used to describe simultaneous heat and mass transfer during drying and baking was proposed by Luikov [30]. The concepts of irreversible thermodynamics and the concept of moisture transfer potential for water movement in a capillary porous body are applied in the model. The Lukov's mathematical model employs the following two assumptions. Pressure gradients within the porous body are very small, and external resistance to heat and mass transfer is negligible [58].

For the present study injera baking is assumed as a contact baking process and the Luikov model and the required simplifications of the model were done based on the physical characteristics of injera baking application, this is as presented in chapter three.

CHAPTER 3

MATHIMATICAL MODELING AND FINITE ELEMENT FORMATION

In this chapter the mathematical model of the heat transfer in injera the bake ware and injera during baking process are presented, the solution of the physical problem is approximated using Finite element discretization of the governing partial differential equation, although there are different FEM formations; this paper followed the gallerkin's method and referred from previous researches on the area of baking [5, 13 and 16]. By making use of reliable assumptions we may reach on the following simplifications.

- The heat transfer process is assumed as a 2 dimensional axisymmetric problem as shown in Figure 3-1.
- Uniform initial moisture and temperature distribution in the injera sample are assumed.
- Two dimensional heat transfers are considered, in the radial and axial direction**.**

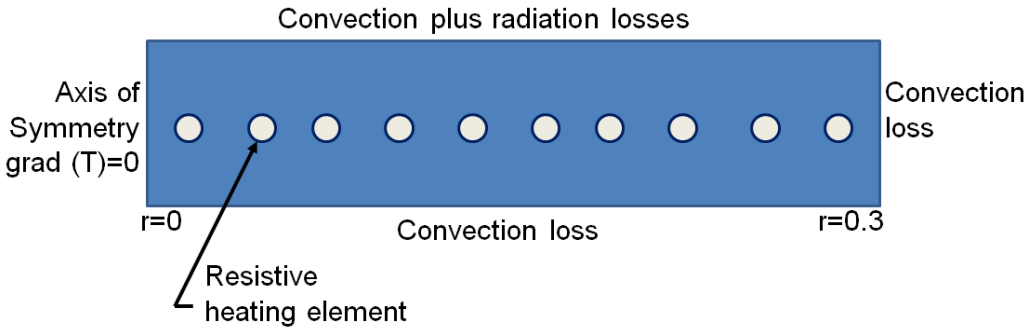

Figure 3-1: *Schematics of the model geometry, axisymmetric representation of a circular baking disk (mitad).*

3.1 Energy Equation for the Bake ware

The partial differential equation for transient heat transfer analysis is given as (Huebneret al., 1995; Kwon, 2000):

$$\rho c \frac{\partial T}{\partial t} = k_r \left(\frac{\partial T^2}{\partial r^2} + \frac{1}{r} \frac{\partial T}{\partial r} \right) + k_z \frac{\partial T^2}{\partial z^2} + Q_A \qquad (3.1)$$

Where: - ρ is density (kg/m^3), c is specific heat capacity (J/kg.k) T is temperature ($^{\circ}$C), t is time (s) and k is the thermal conductivity (W/ m.K). The term Q_A is the heat generation rate per unit area. An initial condition of the bake ware is uniform.

$$T(r, z, 0) = 20^{o}c. \tag{3.2}$$

A general set of boundary conditions for the bake ware both on the top, right side(r=0.3) and bottom surfaces are; as given by Lewis et al. (1996):

$$k\frac{\partial T}{\partial n} + h_c(T - T_a) + h_r(T - T_a) = 0 \tag{3.3}$$

The left side at r = 0, adiabatic conditions are considered due to symmetry about the central z axis.

$$k\frac{\partial T}{\partial r} = 0 \; atr = 0 \tag{3.4}$$

Heat source at the heating coil position is equal to 3kW for a R09 resistor type. For the current ceramic mitad the heating coil is located 1.3 cm from the bottom surface (1.1cm from top baking surface).

3.1.1 Energy Equation during Baking

Heat transfer within the product, injera is treated as a problem of transient heat conduction with phase change that includes evaporation of water.

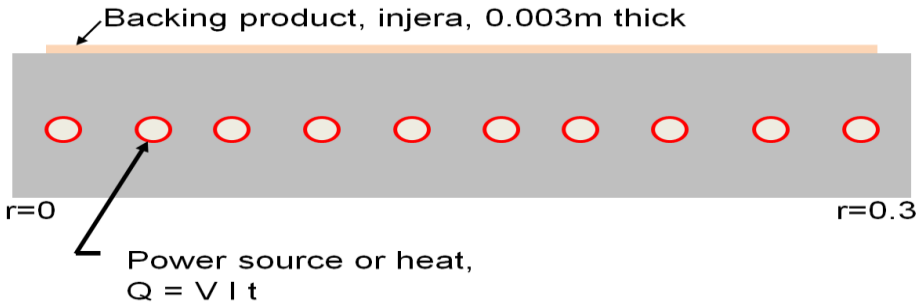

Figure 3-2: *Simplified schematic representation of the injera batter; top, baking disc (mitad) and dimensions for studying the contact baking process.*

Luikov developed a theory of mass and heat transfer for what he called capillary-porous bodies using the principles of irreversible thermodynamics [9],Luikov and his coworkers showed that the thermal and moisture potential gradients within a capillary-porous body cause vapor diffusion and transfer of liquid water. A porous body above freezing temperatures can be considered a moist disperse system consisting of four different

components: a dry porous skeleton (solid), water vapor, liquid water, and air within capillaries and pores. Using the subscript i to denote the i^{th} component (i = 0 for bone-dry solid, i = 1 for water vapor, i = 2 for liquid water, and i = 3 for air), and after neglecting the water vapor and air masses, the mass transfer of bound water can be modeled by the following conservation equation assuming that the moist material can be regarded as a continuum [9]:

$$\frac{\partial(\rho m)}{\partial t} = -\nabla.(J_1 + J_2) \tag{3.5}$$

Where m is the moisture content of the body (dry basis), ρ is the density of the bone-dry Solid, J_i denotes the mass flux of component i, and t is time. The heat transfer within the Material can be modeled by the energy conservation equation. The governing equation during injera baking is derived based on Luikov heat and mass transfer theory. The effect of phase change on the temperature gradient was considered by neglecting the effect of pressure transfer. The mathematical model consists of coupled partial differential equations for simultaneous heat and mass transfer [10, 11, and 15].

The balance of thermal energy with in a capillary-porous body can be described as [10]:

$$\rho c_o \frac{\partial T}{\partial t} = -\nabla.(q) - \left(h_i I_i + h_j I_j\right) \tag{3.6}$$

Where:-C_o is the weighted specific heat of the moist solid referred to as the unit mass of the dry solid, T is the temperature of the dispersed system, q is the total heat flux, Hi is the enthalpy per unit mass, and Ii denotes the mass formation or disappearance rate during the phase changes.

Solutions to (3.5) and (3.6) with appropriate boundary and initial conditions give the moisture and temperature profiles within the material. However, before solving (3.5) and (3.6) with appropriate boundary and initial conditions, the mass flux J_i and the heat flux q should be expressed in terms of driving forces (moisture potentials and temperature gradients). Using the thermodynamics of irreversible processes and experiments, Luikov [9] proved the existence of two driving forces for mass transfer: the moisture concentration gradient and the temperature gradient for each of the mass fluxes. This means that the vapor diffusion and transfer of liquid water within the material can occur due to moisture concentration gradient and/or temperature gradient (thermo diffusion effect). Hence, J_1 and J_2 in equation (3.5) can be replaced by

$$J_1 = -a_{m1}\rho_o \nabla m - a_{m1}^T \rho_o \nabla T \quad (3.7a)$$

$$J_2 = -a_{m2}\rho_o \nabla m - a_{m2}^T \rho_o \nabla T \quad (3.7b)$$

Where: - a_{m1} and a_{m2} are the effective diffusion coefficients for water vapor and liquid, respectively, and a^T_{m1} and a^T_{m2} are the corresponding thermal moisture diffusion coefficients. Substituting this two to equation 3.5 gives:

$$\frac{\partial m}{\partial t} = \nabla.(a_m \nabla m + a_m^T \delta \nabla T) \quad (3.8)$$

Where a_m is the total diffusion Coefficient; $a_m = a_{m_1} + a_{m_2}$, and δ is the thermo-gradient Coefficient given by:

$$\delta = \frac{a_{m1}^T + a_{m2}^T}{a_{m1} + a_{m2}} \quad (3.9)$$

The thermo gradient coefficient is a measure of relative significance of the mass transfer due to the temperatures gradient. The total heat flux q in equation (3.6) is replaced by:

$$q = -k\nabla T \quad (3.10)$$

Where *k* is the thermal conductivity of the moist material and the ($H_1I_1 + H_2I_2$) term is replaced by:

$$H_1 I_1 + H_2 I_2 = -\varepsilon h_{fg} \frac{\partial m}{\partial t} \quad (3.11)$$

Where h_{fg} the specific enthalpy of phase change and ε is is the phase change coefficient .The phase change coefficient ε varies from 0 to 1 as the vapor diffusion increases relative to liquid transfer during drying [11]. After substituting (3.5) and (3.10) into (3.6),

$$c\rho \frac{\partial T}{\partial t} = \nabla.(k\nabla T) + \varepsilon h_{fg} \frac{\partial m}{\partial t} \quad (3.12)$$

For all practical purposes, the heat and mass transfer in a porous body can be simplified in to (3.8) and (3.12). The system of equations given by (3.8) and (3.12) is coupled, and nonlinear PDEs, further assuming constant values for the parameters a_m, c, ρ_o, k, and δ along the spatial dimension the equation can be simplified. Therefore, we seek to solve the following system of equations:

$$\frac{\partial m}{\partial t} = \nabla.(a_m \nabla m + a_m^T \delta \nabla T) \quad (3.13)$$

$$c\rho\frac{\partial T}{\partial t} = \nabla.(k\nabla T) + \varepsilon h_{fg}\frac{\partial m}{\partial t} \tag{3.14}$$

But flat surfaces like the injera having thickness of 0.003m and diameter of 0.58m; it is practical to neglect the effect of change of moisture potential. This means the water content in the batter changes mainly due to the temperature gradient and the effect of moisture potential can be neglected this gives as:

$$c\rho\frac{\partial T}{\partial t} = \left(k + \rho_o \varepsilon h_{fg} a_m^T \delta\right)\nabla^2 T \tag{3.15}$$

Where: - $\left(k + \rho_o \varepsilon h_{fg} a_m^T \delta\right)$ is the effective thermal conductivity of the medium.

The initial temperature and moisture content within injera before baking is assumed uniform and given by:

$$T(r,z,t_o) = T_o = 20_c^0 att = 0 \tag{3.16}$$

$$m(r,z,t_o) = x_{wo} = 73\%\ att = 0 \tag{3.17}$$

And the boundary conditions are:

At the contact between injera batter and mitad energy balance yields.

$$-k\frac{\partial T_p}{\partial n} = -k\frac{\partial T_{inj}}{\partial n} + \varepsilon q_{evap} \tag{3.18}$$

Where $-k\frac{\partial T_p}{\partial n}$ is the heat conduction in the baking disc at the top (z=0.026), $-k\frac{\partial T_{inj}}{\partial n}$is the heat conduction to the injera batter at the bottom (z=0.026). εq_{evap} is the local heat of evaporation of water.

where:- The first term on the left is The heat transfer by conduction from the bottom surface to the inside of the product, the first term on the right is heat penetrating to the product by means of conduction, and the last term is the heat dissipation for the evaporation of water at the interface.

At the top and side surface; the domain is subjected to convection boundary condition, as temperatures of baking of foods in such conditions ($T<100^o{}_c$) the Radiative heat transfer is negligible.

$$k\frac{\partial T_{injTop}}{\partial n} + (1-\varepsilon)h_c\left(T_{top} - T_{inf}\right) = 0 \tag{3.19}$$

Where $T_{injTop}$is temperature of injera, T_{inf} is the outside environment temperature, h_c is the convective heat transfer coefficient and *(ε)* is the phase change coefficient.

Similar to the bake ware the left boundary condition of the injera is adiabatic; due to an assumed symmetry about the vertical axis.

3.1.2 Finite Element Formation of the Governing Differential Equation

Once the governing partial differential equations are obtained from the mathematical modeling, a series of finite element formulations are performed to obtain a numerical solution of the governing partial differential equations using Gallerkin weighted residual method. The finite element equations were formulated based on the methodologies adopted in different literatures [10, 11, 12, and 13].

In many 3D problems there is often a geometric symmetry about a reference axis , and such problems can be solved using 2D elements, provided the boundary conditions and all filed functions are independent of the circumference direction, The domain can then be represented by axisymmetric ring elements and analyzed in a similar fashion as that of a 2D problem.

Considering the heat source boundary at the bottom of the mitad is independent of the circumference and only varies with radius the domain is symmetric about the vertical axis.

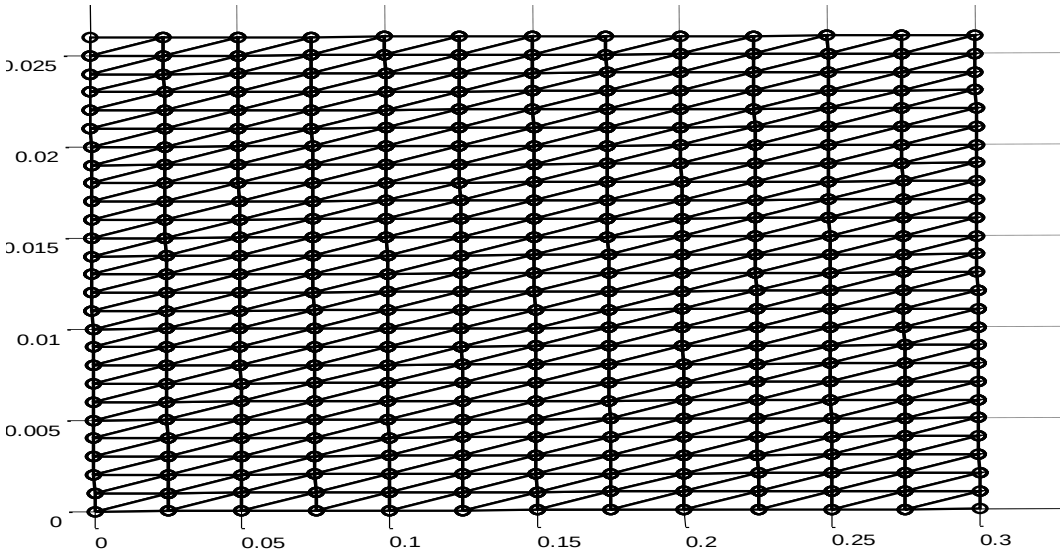

Figure 3-3: *Bake ware Geometry and representation of the ring elements (units are in meter).*

The derived mass matrices, stiffness matrices and force vectors are given below, the detail derivation of the Finite Element Formation were not revised in this study.

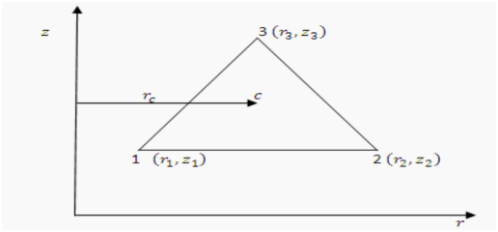

Figure 3-4: *Linear triangular ring element section view.*

Where: A is the area of a triangular element. The element mass matrix is:

$$[C]^e = \frac{1}{\alpha}\frac{A}{60}\begin{bmatrix} 6r_1+2r_2+2r_3 & 2r_1+2r_2+r_3 & 2r_1+r_2+2r_3 \\ 2r_1+2r_2+r_3 & 2r_1+6r_2+2r_3 & r_1+2r_2+2r_3 \\ 2r_1+r_2+2r_3 & r_1+2r_2+2r_3 & 2r_1+2r_2+6r_3 \end{bmatrix} \tag{3.20}$$

The element stiffness matrix is:

$$[K]^e = \frac{r_c}{4A}\begin{bmatrix} b_1^2+c_1^2 & b_1b_2+c_1c_2 & b_1b_3+c_1c_3 \\ sym & b_2^2+c_2^2 & b_2b_3+c_2c_3 \\ sym & sym & b_3^2+c_3^2 \end{bmatrix} + \frac{hl}{3k}\begin{Bmatrix} 0 & 0 & 0 \\ 0 & 2r_j+r_k & r_j+r_k \\ 0 & r_j+r_k & r_j+2r_k \end{Bmatrix} \tag{3.21}$$

Hear the second term after the equality is the contribution to the stiffness matrix due to convection boundaries of the physical domain.

The force vector at convective boundaries is:

$$\{F\}^e{}_h = \frac{hT_\infty l}{3k}\begin{Bmatrix} 2r_i+r_j \\ r_i+2r_j \end{Bmatrix} \tag{3.22}$$

Where r_i *and* r_j are coordinate values of boundary nodes i and j, and l is the side length of triangle element. For a constant rate of heat generation, within the domain at the physical location 1.33 cm from the bottom surface:

$$Q = \frac{\dot{Q}_v}{k}\frac{A}{6}\begin{Bmatrix} 2r_1+r_2+r_3 \\ r_1+2r_2+r_3 \\ r_1+r_2+2r_3 \end{Bmatrix} \tag{3.23}$$

The element equations are then assembled in to the global equation and give the final result as:

$$[C]\left\{\frac{\partial T}{\partial t}\right\} + [K]\{T\} = \{F\} \tag{3.24}$$

$$[C]\{\frac{\partial \dot{T}}{\partial t}\}^{t+\Delta t} + [K]\{T\}^{t+\Delta t} = \{F\}^{t+\Delta t} \tag{3.25}$$

The time derivative in the backward difference technique is:

$$\{\frac{\partial \dot{T}}{\partial t}\}^{t+\Delta t} = \frac{T^{t+\Delta t} - T^{t}}{\Delta T} \tag{3.26}$$

The above matrices are coded in a math lab package; which is used to simulate both the heating up and injera baking processes in the stove; and graphs of cyclic baking results and heat up requirements were studied, the results are given in the next chapter:

The matrices of the injera domain are similarly formed like that of the baking disk, but the conditions of non-linearity are considered while simulating the baking process, temperature dependent properties of the dough were updated each time before predicting the next time temperature of the product.

CHAPTER 4

HEAT TRANSFER COEFFICENTS AND SIMULATION RESULTS

The forth chapter focuses on the determination of the thermo physical properties and the heat transfer coefficients, these are determined analytically as follows:-

4.1 Heat Loss Coefficients of the stove

Heat is lost in three directions of the bake ware; the side, the bottom and top directions of the stove. All the three modes of heat transfers, (conduction, radiation and convection) participate in the transfer of energy to the surrounding. During baking the bottom side of injera is heated by conduction from the top bake ware surface temperature and heat is given off from injera at the top surface to the surrounding by convection. So the energy transferred to injera is accounted as the useful energy used to cook the product and is not considered as a loss.

Heat lost coefficients are the heat transfer coefficients at the three sides of the stove and the heat transfer to the product were not considered as a loss since this is the heat used to cook the product,

The heat source to the bake ware /”mitadʻ/ is the current flow through Ni–Cr coil (or wire) that is imbedded in the groove provided at the bottom side of the bake ware. The bake ware gets heated due to the resistance to the flow of current through the heating element; what is termed as ohmic heating or joules heating.

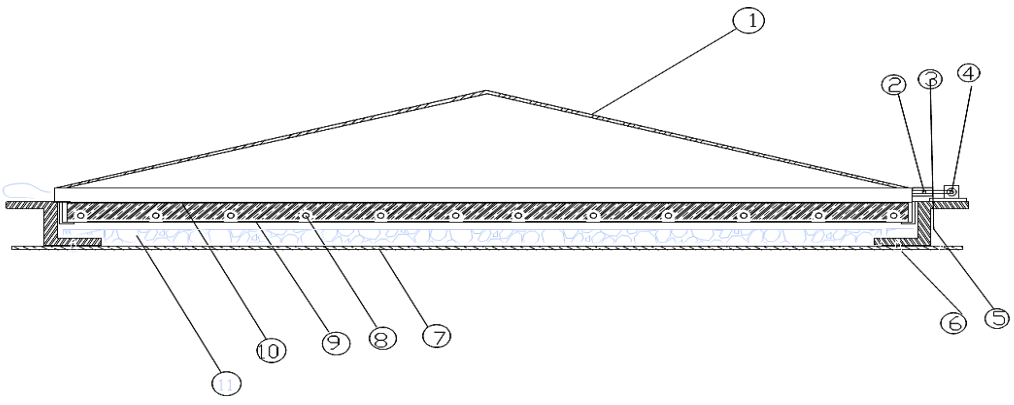

Figure 4-1: *Schematics showing the physical boundaries of the electric stove.*

The above figure and the Labels of the components of the stove are provided in Appendix L.

4.2 Surface Heat Transfer Coefficient

The surface heat transfer coefficient is influenced by the composition of the fluid, the nature and Geometry of the surface, and on the hydrodynamics of the fluid moving past the surface (item 1and 10 in the figure 4.1). From The boundary conditions the heat transfer coefficient over the bake ware is the combined effect of the heat transfer coefficient due to convection and radiation.

$$h = h_c + h_r \tag{4.1}$$

Where h_c convective heat transfer coefficient in (W⁄m2.K), h_r Radiative heat transfer coefficient (W⁄m2.K) and *h is s*urface heat transfer coefficients in (W⁄m2.K).The convective heat transfer coefficient over the bake ware is given by:

$$hc = \frac{N_u . k}{L} \tag{4.2}$$

Where: - *Nu* is the Nusslet Number, *K* is the thermal conductivity of the fluid (w/m. k), *L* is the characteristic length (m).

4.2.1 Convective Heat Transfer Coefficient

In the determination of convective heat transfer coefficient a dimensionless functional Relationship derived using dimensional analysis between h_c and the relevant physical properties of the flow situation are used**.** The functional of this relationship is given by:

$$hc = f(\rho, V, L, \mu, cp, \Delta T, k, \beta, g) \tag{4.3}$$

Where ρ is Density of fluid (kg/m^3), *V* is Average fluid velocity (m/s), *L* is Characteristic length (m), μ is Dynamic viscosity (N.s/m2), c_p is Specific heat of fluid (J/kg. k), β is volumetric expansion coefficient (1/k), g is Gravitational acceleration (m/s2). By performing a dimensional analysis on the above equation, the following functional relation can be derived*:*

$$\frac{hcL}{k} = f\left(\frac{\rho VL}{\mu}, \frac{c_p \mu}{k}, \frac{\rho^2 g \beta L^3 \Delta T}{\mu^2}, \frac{V^2}{c_p \Delta T}\right) \tag{4.4}$$

Where: - $Ra = \frac{\rho VL}{\mu}$ is the Reynolds number, $pr = \frac{c_p \mu}{k}$ is the Prandtle number, $Gr = \frac{\rho^2 g \beta L^3 \Delta T}{\mu^2}$ is the Grashof number and $\frac{V^2}{c_p \Delta T}$ is the Eckert number. In natural convection, many correlations contain the product of the Grashof number and the Prandtle number; the product of the two is defined as the Rayleigh number:

$$Ra = Gr * pr \tag{4.5}$$

As the motion of fluid in free convection is caused by buoyancy force, for horizontal plates either from the plate or toward the plate, two situations should be distinguished. First, heat transfer occurs in the direction of gravitational force (lower surface heated upper surface cooled), and second, heat transfer against the direction of gravitational force (Upper surface heated lower Surface cooled).A general correlation between the Musset number and Rayleigh number is developed based on the above two cases as:

$$Nu = C(Gr * Pr)^m \tag{4.6}$$

Where, *m* and *C* are constants .The value of the constants depends on geometry. Since heat transfer during injera baking is against the direction of gravitational force, only the second case is used for this study. Fuji and imura (1972) proposed the following correlation for heat transfer to or from the horizontal plate with constant heat flux [19, 41, 42, and 48]:

$$u = 0.13(Gr * Pr)^{\frac{1}{3}}, \qquad for Gr * pr < 2 * 10^8 \tag{4.7a}$$

$$Nu = 0.16(Gr * Pr)^{\frac{1}{3}}, \qquad for\ 2 * 10^8 Gr * pr < 10^{11} \tag{4.7b}$$

β is evaluated at $T_\infty + 0.25(T_s - T_\infty)$and all other properties at$T_s - 0.25(T_s - T_\infty)$, T $_s$is average wall temperature. Correlations are also presented for flat surfaces without constant heat flux as, [19, 41, 42, and 48]:

$$Nu = 0.54(Gr * Pr)^{\frac{1}{4}}, \qquad for 10^4 < Gr * pr < 10^7 \tag{4.8a}$$

$$Nu = 0.15(Gr * Pr)^{\frac{1}{3}}, \qquad for 10^7 < Gr * pr < 10^{11} \tag{4.8b}$$

To determine the convictive heat transfer coefficients of the bake ware air properties are first evaluated at the average film temperature. This is the average temperature between the bake ware top surface and the temperature of the environment.

$$T_s = \frac{T_s + T_\infty}{2} = \frac{200 + 20}{2} = 110_c^o \tag{4.9}$$

The film temperature to evaluate the properties of air is *Tw = Ts-0.25*($T_s - T_\infty$)* = 110-0.25*(200-20) = 87.5°c. Air properties are calculated at the average film temperature and are summarized in Table 4-1:

Table 4-1: *Air properties at average film temperature.*

Density, ρ	β	pr	μ	ν	k	C_p
(kg m^{-3})	(K^{-1})	()	(kg $m^{-1}s^{-1}$)	(m^2 s^{-1})	(w $m^{-1}K^{-1}$)	(J kg^{-1} K^{-1})
0.996	2.77×10^{-3}	0.71	2.12×10^{-5}	2.22×10^{-5}	0.035	1010

The characteristics length for circular disk is experimentally approximated as L=0.9D [19, 42], Where D is the diameter of the bake ware. The dimensionless Grashof and Rayleigh numbers become:

$$Gr = \frac{\rho^2 g\beta L^3 \Delta T}{\mu^2} = 7.85 * 10^8 \tag{4.10}$$

$$Ra = Gr * pr = 5.57 * 10^8 \tag{4.11}$$

Using equation 4.7b

$$Nu = 0.16(Gr * Pr)^{\frac{1}{3}} = 131.69 \tag{4.12}$$

This gives the convective heat transfer coefficient from bake ware to lid cover; h_{1C} is calculated to be 7.445 W. $m^{-2.}$ K^{-1}. And the convection heat transfer coefficient from lid cover to ambient, h_{2C} is equal to 14.8 W. m^{-2} .K^{-1}.

4.2.2 Radiative Heat Transfer Coefficient

The Radiative heat transfer coefficient at the surface of the bake ware is given by:

$$h_r = \delta * \varepsilon * \left(\frac{T_s^4 - T_\infty^4}{T_s - T_\infty}\right) = \delta * \varepsilon * (T_s^2 + T_\infty^2) * (T_s - T_\infty) \tag{4.13}$$

Where δ is Steffen Boltzmann constant (5.67 ×10^{-8}W $m^{-2}k^{-4}$), and$\mathcal{E}$ is the emissivity of the surface (0.95).Substituting the values to the above equation the Radiative heat transfer coefficient, $h_{r,}$ becomes 8.47 W m^{-2} K^{-1}.

4.2.3 Total Heat Transfer Coefficient

The total surface heat transfer coefficient on the top surface of the bake ware is the combined effect of the radiation and convection heat transfer coefficients from the bake ware and the lid cover as given by Eqn. (4.1) and a value coated on previous research on the same body of the stove used for the preset is used; which equals to 15.45 W m^{-2} K^{-1} .During injera baking as the temperature of the food doesn't exceed 100^{o}c the Radiative heat loss is neglected, and only the convective heat transfer from the product were considered, the value of 8W/m^2.k for most baking applications were used.

4.3 Bottom Heat Transfer Coefficient

Heat is lost from the plate to the ambient by conduction through the insulation of the plate casing and subsequently by convection and radiation from the bottom casing surface to the ambient. The total heat transfer coefficients from the bottom casing surface to the ambient is given as:

$$h_b = h_{rb} + h_{cb} \qquad (4.14)$$

The gypsum insulation is taken into account in the calculation, the values coated hear is taken from previous research on the area [5] and the value is 11.8W/m^2.k:

4.4 Lateral or Edge Heat Transfer Coefficient

since the stove casing and side and bottom insulations used are similar to that used in previous tests [5].In this thesis the edge heat transfer coefficient was coated from the previous results which is 7.15 w/m^2.k as coated in [5].Where: Insulation thickness at bottom side is 4mm gypsum board, thermal conductivity of the insulation is 0.2w/m^2.k as reported in many literatures.

4.5 Determination of Thermo physical Properties of Injera

Thermo–physical properties of injera were determined from its major components and temperature Dependent equations reviewed in chapter two, the determined specific heat; thermal conductivity, density are tabulated in appendix E .for the estimation of thermal conductivity the volume fraction were first calculated as shown in appendix E and the average values of the parallel and series models were taken for this study.

Table 4-2: *Thermal properties of the product injera at average temperature (50^oC)*

properties	**Property values**
C_p(Specific Heat, j/kg.k)	3440.07
ρ (Density, kg/m^3)	1160.55
Thermal conductivity(W/ m.k)	0.665

4.6 Moisture Diffusivity

There is no standard method for the determination of moisture diffusion and thermo-gradient Coefficient. Therefore, average values obtained from literatures are used in this study. Moisture Diffusion coefficient between water vapor and air at a standard pressure and temperature is equal To D=0.288×10-4[20], and latent heat of evaporation of water hfg=2256.97 kj/kg. The thermo-gradient coefficient has less influence on the temperature predictions. The value of the thermal gradient coefficient (δt varies from 0.01/c up to 0.02/c) for food products. There is very little published data concerning the value of the ratio of water evaporation rate to the reduction rate of the moisture content during the baking of foods, therefore the value obtained from the literatures [2, 46,], ε=0.3 is used for injera.

4.7 Results of Numerical Simulation

The heat transfer in the bake ware were simulated using estimated boundary heat transfer coefficients at the boundaries of the physical domain and the finite element model was coded in a Math lab m file. This helps to optimize the process for the best efficiency and reliable operation scenarios.

4.8 Power Utilization Scheme

The power input to the bake ware or mitad was achieved by R09 type Nicrome resistance wire, which is commonly used for injera baking stoves. Using ohms law relation as given in equation 2.1 to 2.4:

$$Q = I^2Rt \tag{4.13}$$

$$R = \mathrm{L}\rho/\mathrm{A} \tag{4.14}$$

As in can be seen from the two equations the Electrical energy input to the wire depends on three parameters for a maintained terminal voltage of 220V; it directly depends on the square of the current, the resistor and the time of operation and the resistor depends on the diameter and length of the heating element used and also depends on the temperature of the wire as described in Equation 2.4.

In this paper two R09 types Nicrome resistors of each rated with 1500W capacity and 70cm length were selected and tightly connected at one end and then the wire is uniformly stretched to a length that fit in the grove space provided at the bottom surface of the ceramic bake ware, these arrangement uniformly distribute a total of 3000W resistor wire over the groove space provided.

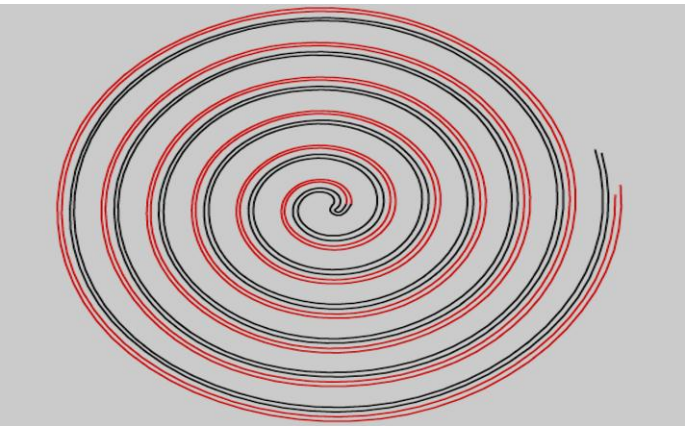

Figure 4-2: *Six turns of double spiral grove at the bottom of the bake ware.*

The resistance of the heating element to the flow of current increases as the temperature of the wire increases: as described in equation 2.3.

The power distribution in each loop is estimated and tabulated in the Table 4.5; this distribution of power was used for the simulation of the actual heating process. It is a common practice to define a new parameter called power density, which is the total power divided by the heated surface area.

4.9 Power Density:

The power density for the bake ware was calculated as, the total power divided by the heated surface area:

$$P_d = \frac{P_{total}}{A_{total}} \tag{4.17}$$

Where: P_d is the total power density. P_{total} is the total power demand which is 3000W; A_{total} is the bottom heated surface area of the bake ware. With an area of 0.269 m^2 the power density is 11.152 Kw/m^2. The total power density is then distributed in each loop based on the following relation taking in to account the area occupied by every loop: the figure shows for the single spiral loop, there are two loops of six turns each.

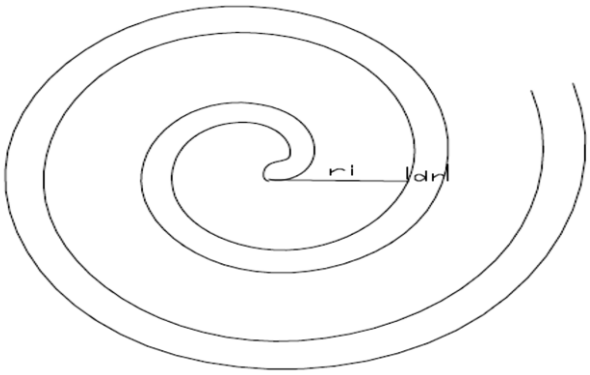

Figure 4-3: *Schematics of the loop area*

I.e. the area occupied by the ith loop in the bake ware is calculated as:

$$A_i = 2 * \pi * r_c * dr$$

Where: r_C is the location of the centroid of the linier triangular element used while forming the finite element model in chapter 3. And dr is the grove width in meter. So, the power in the ith loop is:

$$P_i = A_i * P_d$$

The table below shows the power distribution shame in each loop and in the simulation this power is shared in the element with a ratio proportional to the ratio of the shape function at that location of the source.

Table 4-3: *The power distribution in 10 loops over the three nodes of an element 3KW source*

	node 1	node 2	node 3	Or at one node
1	6.8899	6.8899	6.8899	20.6697
2	27.5596	27.5596	27.5596	82.6788
3	48.2293	48.2293	48.2293	144.6879
4	68.899	68.899	68.899	206.697
5	89.5687	89.5687	89.5687	268.706
6	110.2384	110.2384	110.2384	330.7151
7	130.9081	130.9081	130.9081	392.7242
8	151.5778	151.5778	151.5778	454.7333
9	172.2475	172.2475	172.2475	516.7424
10	192.9172	192.9172	192.9172	578.7515

The table shows the power distribution used in the simulation, the horizontal values in every row is the values at the three nodes of the element, and the column is the number of the elements, or a second approach is to put a node at a location where the source are located. The fifth colon follows this, and the simulation is based on the second approach as it closely approximates the physical locations of the sources in the body.

4.10 Heat Up Time and Cyclic Baking Simulation Result

The heat up time is the time required to heat the bake ware to the temperature needed to commence baking of injera, the required top surface temperature is 180^{o}c to 200 for the conventional clay bake ware as reported by previous researches [4, 6 and13],. The domain of the baking disc (mitad) is discretized in to 624 linier triangular elements to study the heat flow characteristics in the new ceramic mitad; this is seen in figure 4.4.

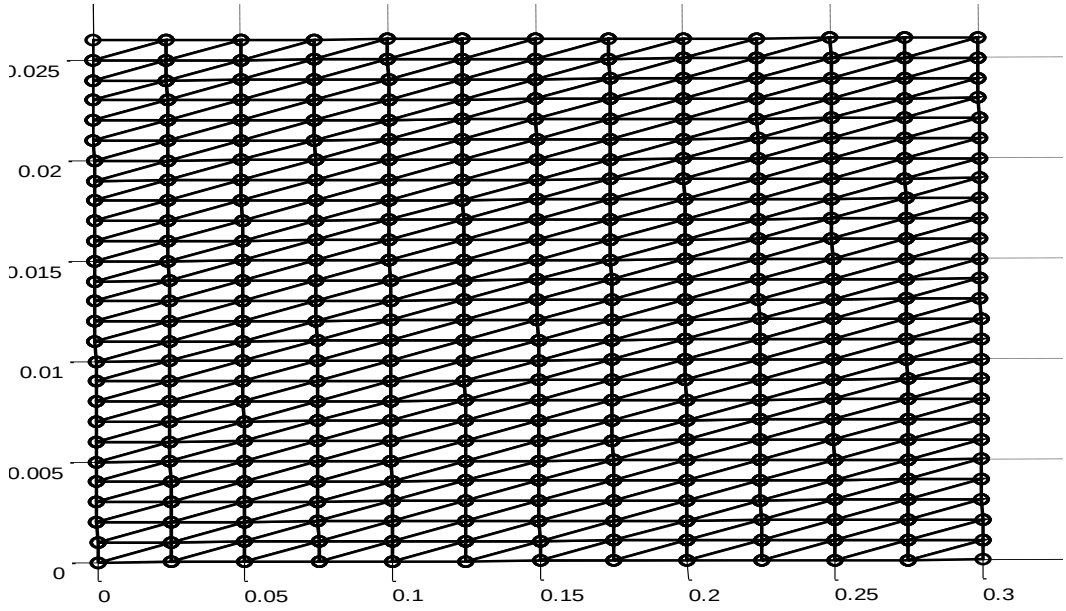

Figure 4-4: *Triangular mesh of the baking disk domain (units are in meter)*

The heat up time taken to bring the mitad top surface temperature to 180 to 200 ^{o}c were simulated for the current geometry of the ceramic mitad; since the current new ceramic mitad has a thickness of 2.6 cm the time is expected to be greater than those having smaller thicknesses of 2cm, 1 cm and 0.8 cm used later to simulate efficiency optimization of the baking disk. The next figure shows the heat up time for the ceramic bake ware that is used for the experimental investigation in chapter 5.

4.11 Heat up Time Simulation Result

Heat up temperature history of the new bake ware /"mitad"/ shows the heating of the mitad from ambient temperature to bake ware surface temperature of (180 ^{0}C, before baking commences). To achieve 180 ^{o}C to200 ^{o}C on the surface of the new bake ware it needs around 1200 –1250 seconds. And the electric power density was around 11.152kW/m^2 of the bake ware surface area. The following two figures show the heat up time for the ceramic and clay bake wares; the increased heat up time of the new ceramic bake ware is mainly due to the larger thermal inertia of the ceramic bake ware used in the simulation. The same dimension of the bake ware is used during experimental investigation in chapter 5.

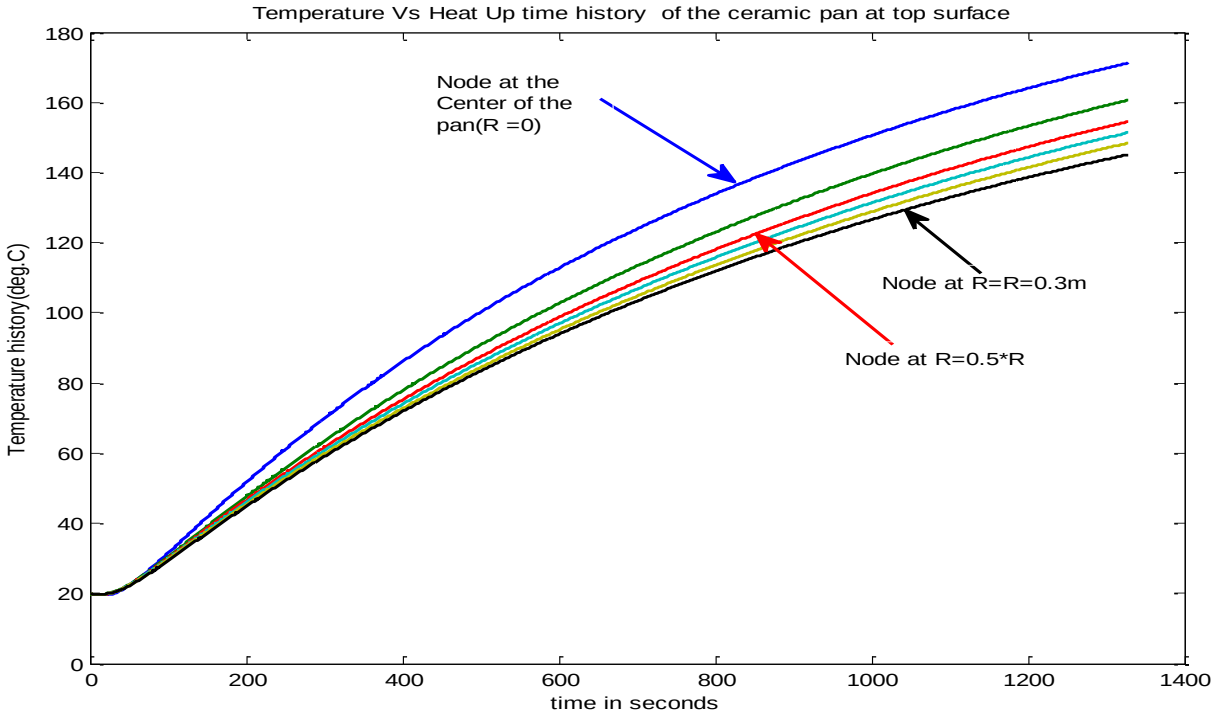

Figure 4-5: *The temperature time history at the surface of the ceramic baking disk.*

Top surface temperature of the bake ware reaches baking temperature at around 1250 seconds of heat up time,with a power input of 3KW. The corresponding heat up times in a clay baking disk is as shown bellow.

The thermophysical properties of clay and ceramic used for the simulation are , k=0.5W/m^2.k,C_p=830 j/kg.k and ρ = 1900kg/m^3 for clay and k=0.95W/m^2.k,C_p=960 j/kg.k and ρ = 2400kg/m^3 for the ceramic material as given in [4].

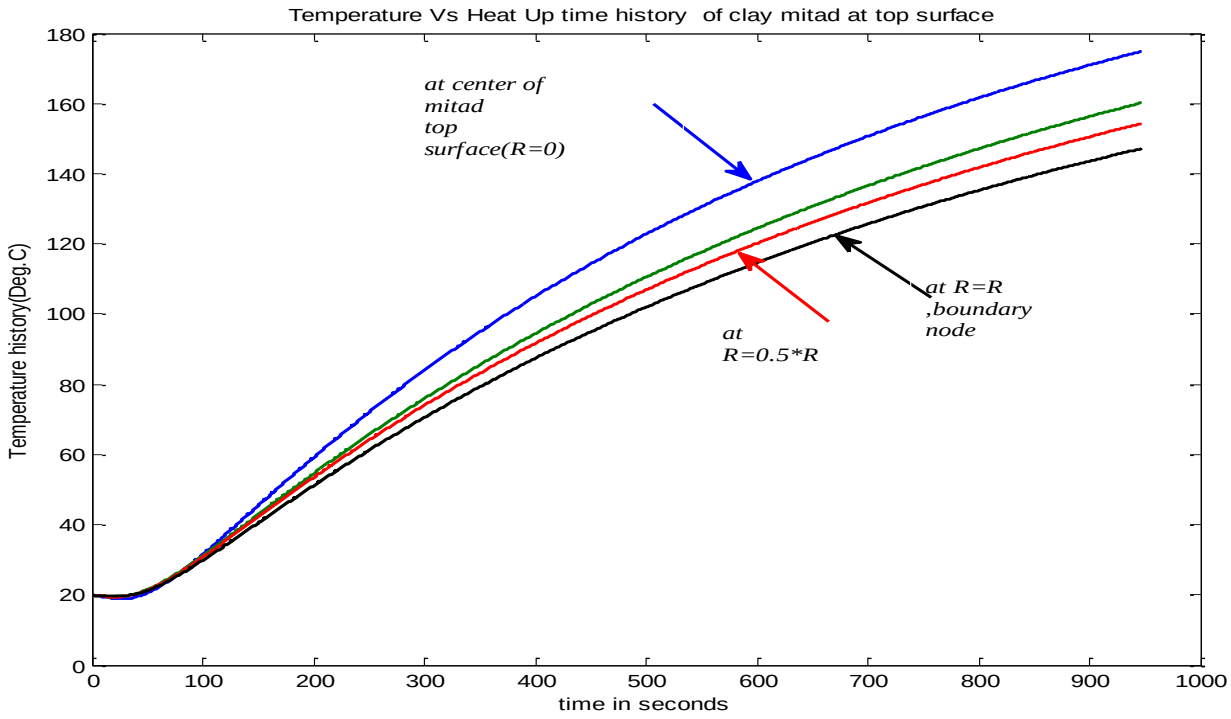

Figure 4-6: *The heat up time for the 3kW power source. It takes 900s to reach a baking temperature of180°C for the conventional clay mitad.*

4.12 Cyclic Baking Simulation Result

The next two figures shows the temperature time history both for the clay baking disk and the new ceramic bake ware including cyclic baking times with the same thickness and power source.

The temperature profile in figure 4.7 and 4.8 shows the temperature at selected nodes across the thickness of the baking disk and the product injera. The figure shows the variation of the temperature at the center at half the radial length and at radial end at eleven nodes selected along the thickness of the bake ware.

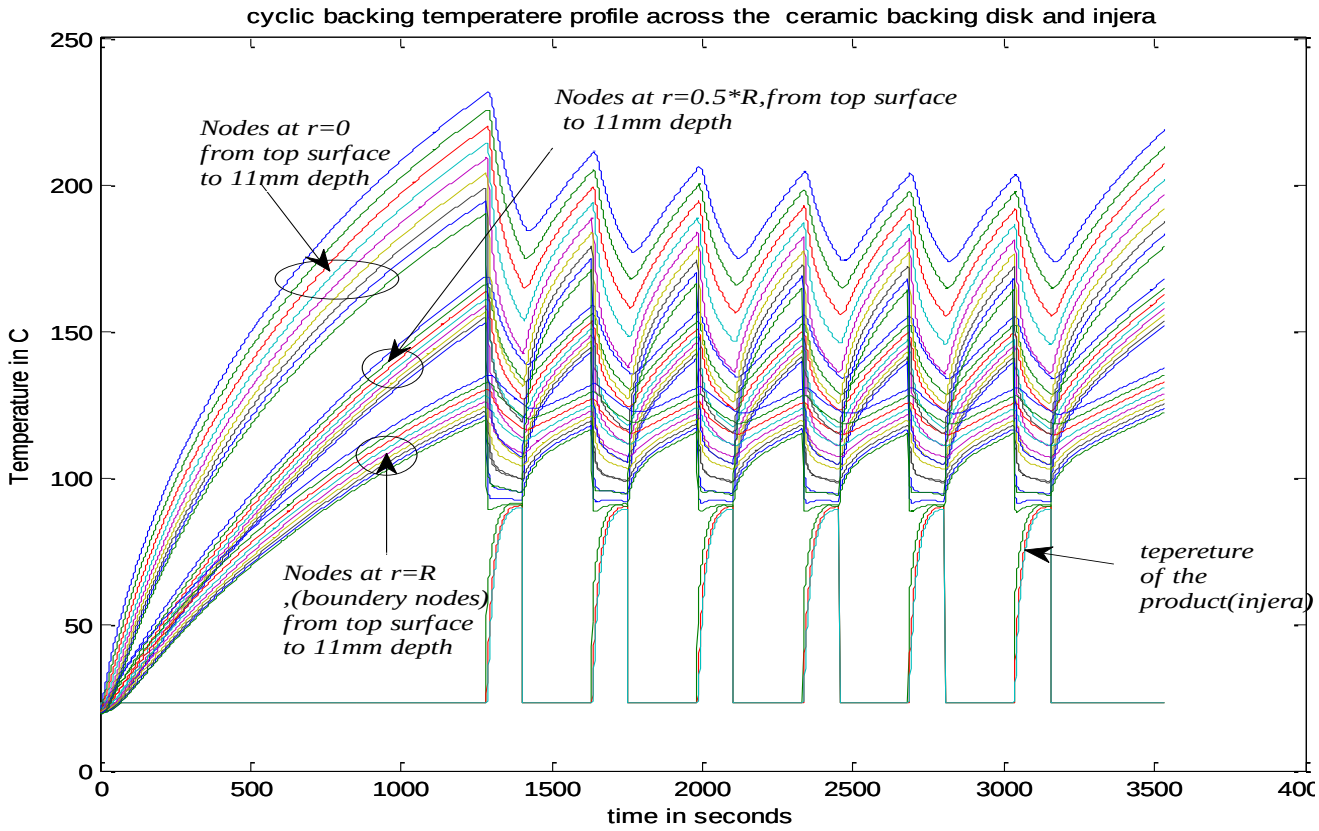

Figure 4-7: *Cyclic baking in the 2.6cm thick new ceramic bake ware.*

It takes longer heat up period and idle heating times, with 23 to 24 minutes of heat up time and 290 seconds of idle heating times; with baking time of 120 seconds per injera; the temperature history at three locations are shown, at the center of the pan , at half the radial distance and at the location of boundaries. Eleven nodes across the thickness were selected at the three locations; its seen that the temperatures are greater for the nodes at the center and lower at the radial end thermal boundary locations as expected due to convection losses at this points. The bottoming profile sows the temperature variation of the product injera.

As it can be seen from the temperature profile the ceramic bake ware (the new bake ware) results in a relatively even temperature distribution and lower temperature gradient in the body during heat up period as compared to the clay mitad in figure 4.8 .And the entire cross section of the ceramic bake ware evenly responds to the changes in the boundary condition due to baking and consumes larger energy both to heat it up to the baking temperature and subsequent idle heating times. I.e. it takes longer time to heat a material to a specified temperature having a relatively higher heat capacity than the one with a lower heat capacity value.

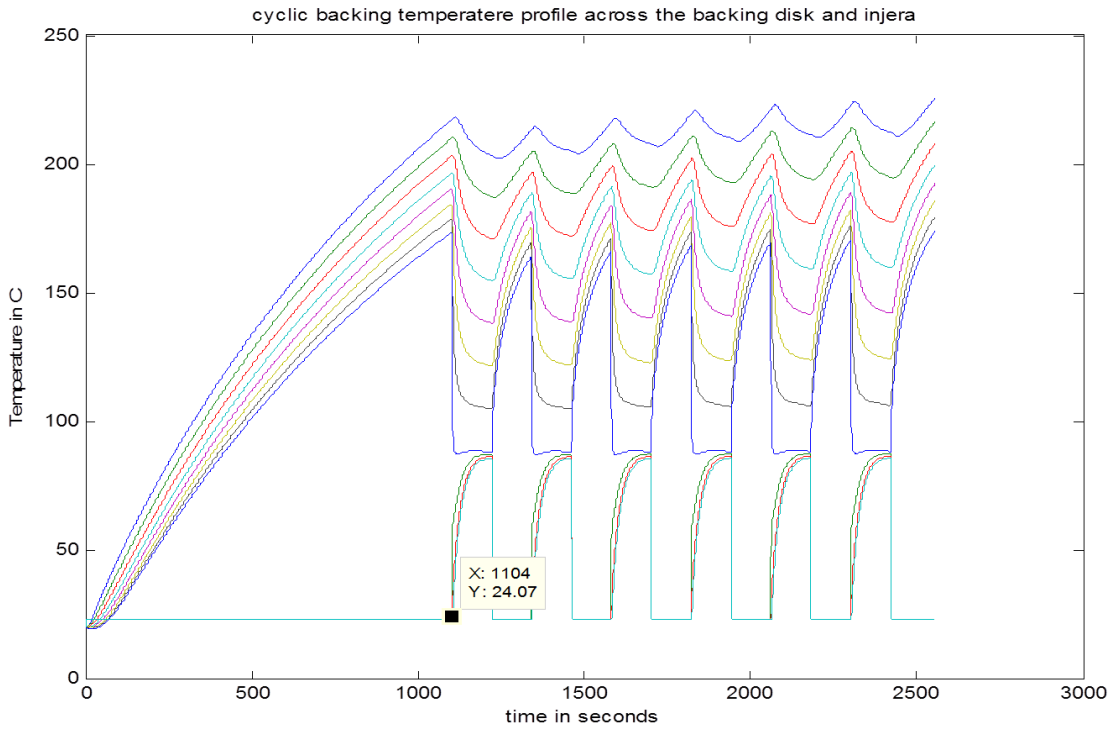

Figure 4-8: *Six cycles of baking temperature profile across the clay baking disk and injera for a 3kW power source.*

Hear the temperature profile of the clay mitad is sown only at half the radial distance , Compared to the ceramic bake ware; the clay bake ware shows lower heating periods (16 minutes) and subsequent idle heating times of 156 seconds. It is seen that the clay body results in a relatively non-even temperature distribution compared to the ceramic bake ware. According to the simulation result; the clay bake ware yields a less energy intensive operation compared to the previous ceramic bake ware. Both are compared with the same geometry, heat transfer boundary conditions and power supply. The clay bake ware needs less heat to recover the top surface temperature to 180^{o}c.

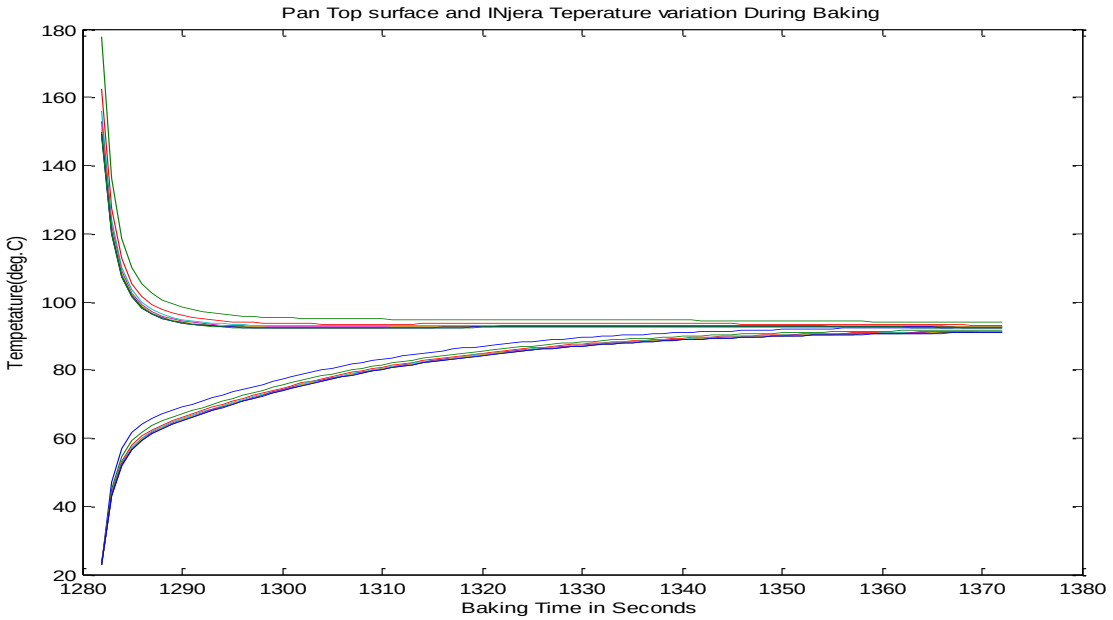

Figure 4-9: *Temperature profile of the injera and ceramic baking disk at the top surface for the 3kW power source.*

The current flow through the heating element was estimated using ohms law and the temperature dependence of resistance of the element as given in equation 2.4. The next graph shows the current flow with the time period of operations.

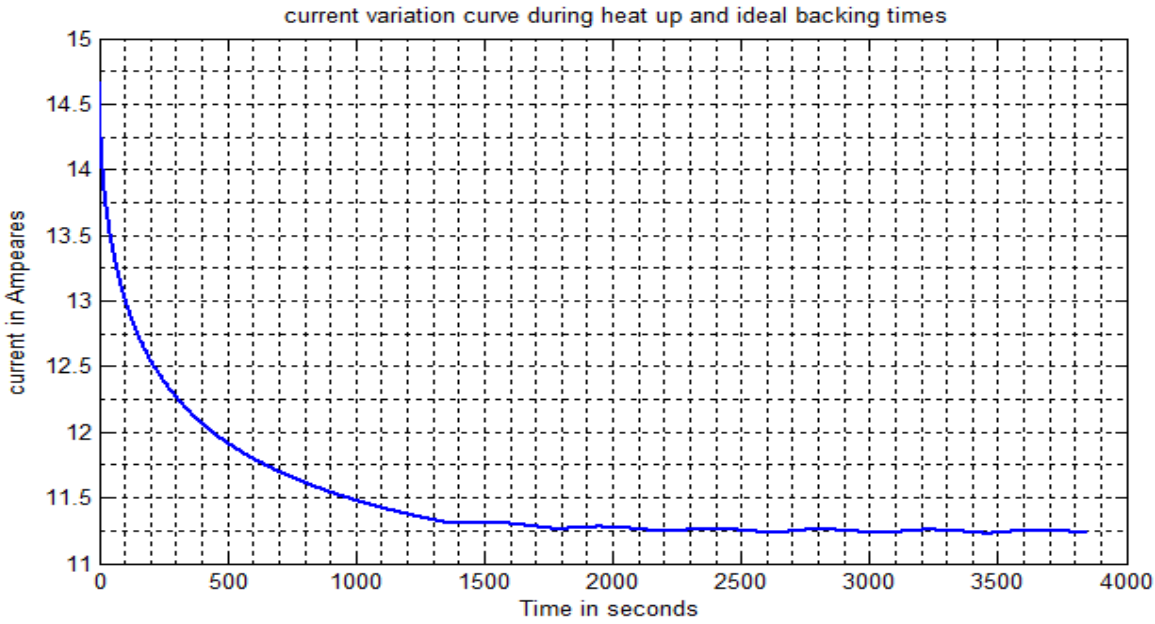

Figure 4-10: *Current variation in the heating element during heating and baking period.*

The initial current flow in the heating element was 15 Amperes obtained from ohms law and the cold resistance of the heating element with an assumed constant voltage of 220 V and current at baking periods is 11.2 Amperes. As the resistance increases in the heater due to increased temperature the current must reduce so that the product R*I = 220 V (the constant terminal voltage). The power is expected to vary in the similar fashion; the power variation is as shown below.

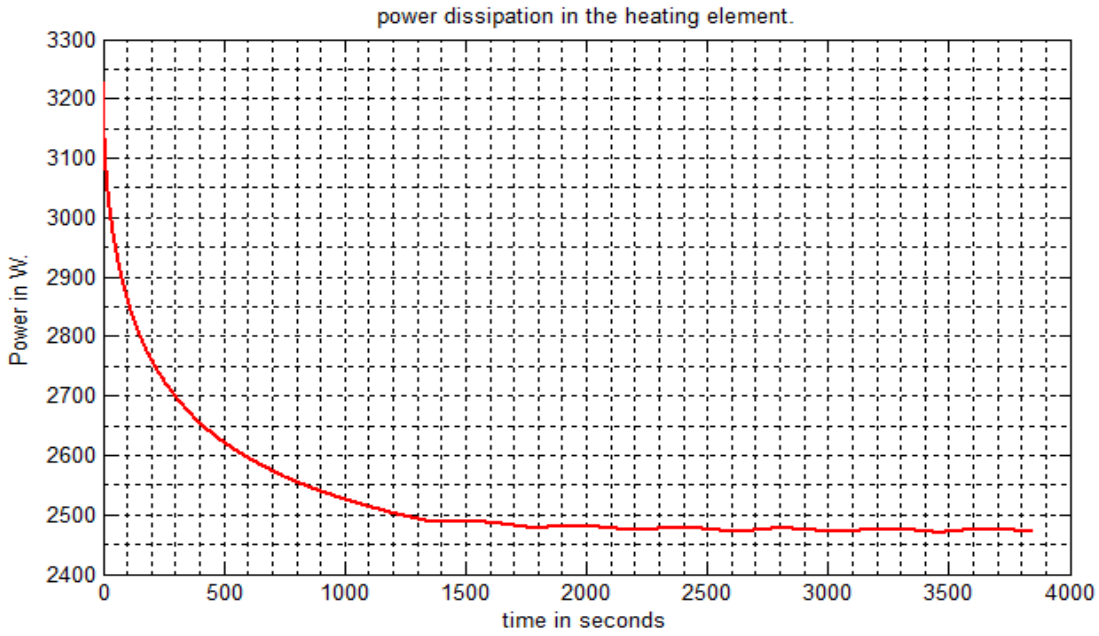

Figure 4-11: *The dynamics of the power dissipation with time of the heating element.*

The power dissipation varies in a similar fashion as the current it varies from 3.2 KW to 2.45KW; this shows as the heating element gets hotter the power dissipation decreases to a value which depends on the temperature of the heater. The cooler the wire is the higher power dissipation and the hotter the wire is the lower the power dissipation. This indicates efficient insulation not only reduces the heat loss but also helps to keep the wire hot and reduce the power dissipation rate in the heater, the main reason for the increase in efficiency with increase in number of injera baked.

4.13 Energy Consumption of the Bake Ware

The energy consumption of mitad depends mainly on its thermal conductivity, heat capacity and thermal diffusivity. The thermal conductivity and thermal diffusivity also influences the heating up time of the utensil. Here below calculated is the energy consumption of the bake ware. For the bake ware the heating up time and the baking temperature of injera is found through field testing, chapter 5.

Basic Data about Injera (from field testing results in chapter 5 and Table 2.1, 4.2**)**

- Mass of one Injera 413.5gm, Average number of Injera for one family at one session is taken as 10.
- Mass of dough(499.5gm) for 10 Injera is 4.995kg (72.6% of it is water and 27.4% of it is teff)
- Cp of teff is 3.44KJ/Kg ^{o}K [Table 4.2], Baking temperature of Injera = 180^{0}c-210^{0}c.
- Mass of water that evaporates during baking =mass of liquid dough – mass of injera = 499.5gm -413.5gm = 0.0865 kg.
- Moisture content of injera, 58 to 60 %.

About bake ware.

- Diameter of bake ware = 58.50 cm, Thickness of mitad = 2.6 cm, Mass of Mitad average = 12.5kg
- Cp of ceramic Mitad 0.96KJ/Kg [Table 2.1],
- Thermal conductivity of ceramic mitad 1.27 W/m K other accessory data [Table 2.1].
- Time needed for the ceramic bake ware to reach the electric bake ware (ceramic) from room temperature to cooking temperature is 20.5min.
- Time needed to bake one Injera 2 min (120 seconds), the time gap between successive Injera baking is 120sec.

$$Q_{total} = Q_{heat\ up} + Q_{backing} \tag{4.16}$$

For ten baking cycles the simulation gives a total of 8.6163Mj of electrical Energy input to the stove.

4.14 Energy Utilized for Baking and Baking Efficiency.

From field recording of the moisture, initial and final masses of the product injera the energy actually utilized for baking the 10 injera was 3.63MJ; calculated in chapter 5. As described in chapter 2 the efficiency of the bake ware is the ratio of the energy used for baking to the total heat used to heat up the bake ware and subsequent cyclic baking's.

$$\eta = \frac{E_{cook}}{\dot{Q}_{heat} * time} \quad (4.18)$$

Where

$$E_{cook} = m_{injera} \times c_{pinjera} \times (T_{boiling} - T_{initial}) + n_{cycle} \times \Delta m_{moist} \times h_{fg} + \Delta m_{moist*(T_{boiling} - T_{initial})}$$

T_{total} = *heat up time + ncycle × cooking time+ (ncycle-1)× idle heat up time.*

where $E_{cook}$is the energy utilized for baking, the sensible heating of injera and latent heat of evaporation of moisture, $\Delta m_{moist}$is the change in moisture of injera during baking, $m_{injera}$is the mass of injera on a dry basis, $n_{cycle}$is the number of cooking cycles, $\dot{Q}_{heat}$ is the power used in watts, t_{total} is the total time of heating. The efficiency of the baking disk is calculated from the above relation and values from chapter 2 for the thermo-physical properties and mass of injera and the change in moisture of the product, and the efficiency for different cooking cycles is as shown in the table 4.4.

Table 4-4: *Energy consumption and Efficiency of cooking for two power inputs and different cycle of baking for 0.008m thick ceramic bake ware*

Power	Baking cycles	Total time (sec)	Energy input (MJ)	Energy utilized (MJ)	Efficiency (%)
2.2KW	10	3196	5.15	6.93	74.4
	15	4521	9.965	7.73	77.58
	20	5846	13.01	10.31	79.3
3KW	10	2335	6.7	5.154	79
	15	3311	9.64	7.73	80.2
	20	4286	12.6	10.31	82

Reducing the power to 2.3KW results in a reduced efficiency of cooking due to an increased period of the corresponding heat up, baking and idle time heating's, for the 2.3KW power source the baking time is 110 seconds and idle time heating is 175seconds.But the 3KW power source provides a baking time of 90 seconds and idle heat up time of 105 seconds and also a reduced heat up period of 400seconds. But the heat flow rate sufficient for slow cooking application has to be considered when trying to enhance the efficiency of cooking. So, it is preferable to keep the resistor length to the 12m and the power to 3KW to obtain an

increase in efficiency of cooking. It is also evident that increase in the number or baking cycle also increases the efficiency of baking. For 50 cycles of baking on the 3KW power supply provides 86% efficiency.

To measure the performance index of the current mitad the total Energy intensity for ten cycles of baking was calculated and yields 2.07Mj/kg.

4.15 Calculation of Thermal Stress Due to Temperature Gradient

Assuming free expansion of the body at the boundaries as described in chapter 2, only the stress due to temperature gradient and sudden cooling effects are estimated. The stress at the location of source of heat and the stress at the top surface at the end of heat up time are calculated using equation 2.9 and the radial variation of tensile stress is shown below.

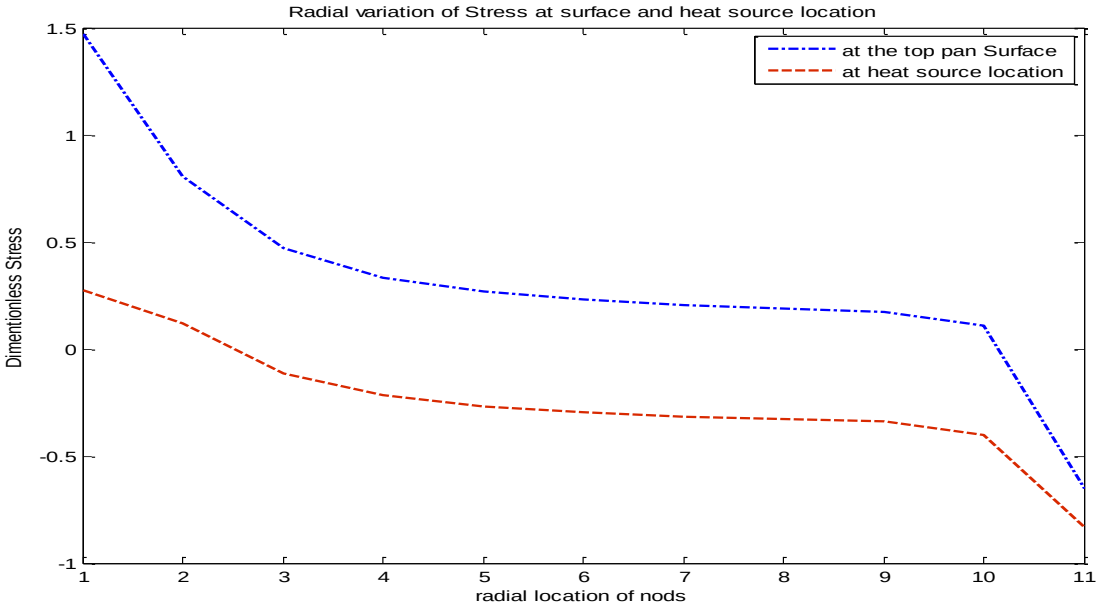

Figure 4-12: *The dimensionless stress vs. radial location of nods at heat source and top bake ware locations.*

At both locations the stress is calculated with respect to the mean temperature in the body; it is found that the stress decreases at the top surface and radial end locations, this difference in stress may create difference in free expansion of each volume elements in the body and eventually may be the cause of weakening of the body and crack to form.

As the circumferential ends are the thermal boundaries of the domain, the temperature are lower than the central regions; hence there is a variation of temperature at any time during operation, this variation of temperature creates a radial stress gradient and may causes

separation of the edges from the central body due to different in expansion. This result suggested there should be sufficient insulation of the bake ware at the sides with a non-rigid insulation material like fiber glass.

4.16 Estimation of Tensile top surface stress due to Sudden Change in Temperature

Cooling of the top surface of the ceramic body occurs relatively at a faster rate, the tensile top surface stress developed due to baking is estimated using equation 2.9 from the temperature distribution of the bake ware. The sudden variation of top surface temperature and the tensile stress are shown in the following two figures.

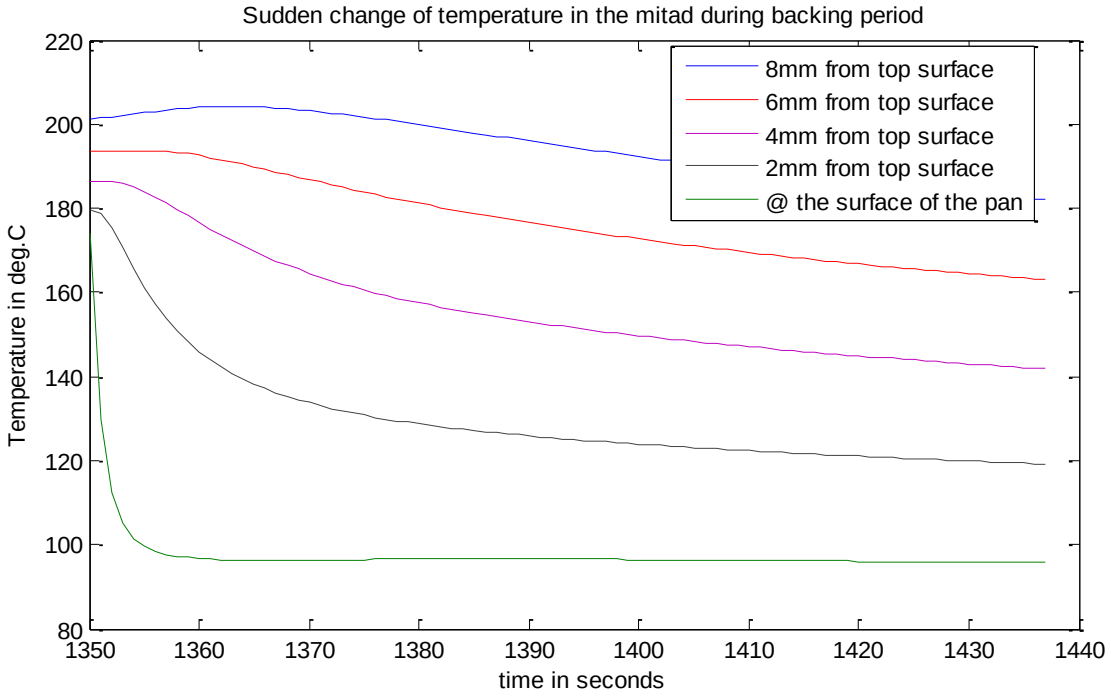

Figure 4-13: *Sudden change in temperature across the mitad during baking period.*

The corresponding cyclic tensile stress development in the mitad is simulated for thermoplastic properties taken from literatures written on ceramic materials [21]. Figure 4.14 shows the non-dimensional stress variation across the thickness of the mitad; the cyclic tensile stresses at or near the location of the source are well below the maximum fractural stress of the ceramic body but sections towards the top surface of the mitad yields a tensile stress above the value of the fractural stress. As it was described in chapter 2; during baking time the section of the mitad above the heat source experiences tensile stress while the ceramic body at the location of the heat source always in compression. These cycles of

heating and cooling; hence cycles of contraction and expansion at the top surface relative to the rest of the body may results in wakening and crack formation at the top surface and may eventually leads to failure.

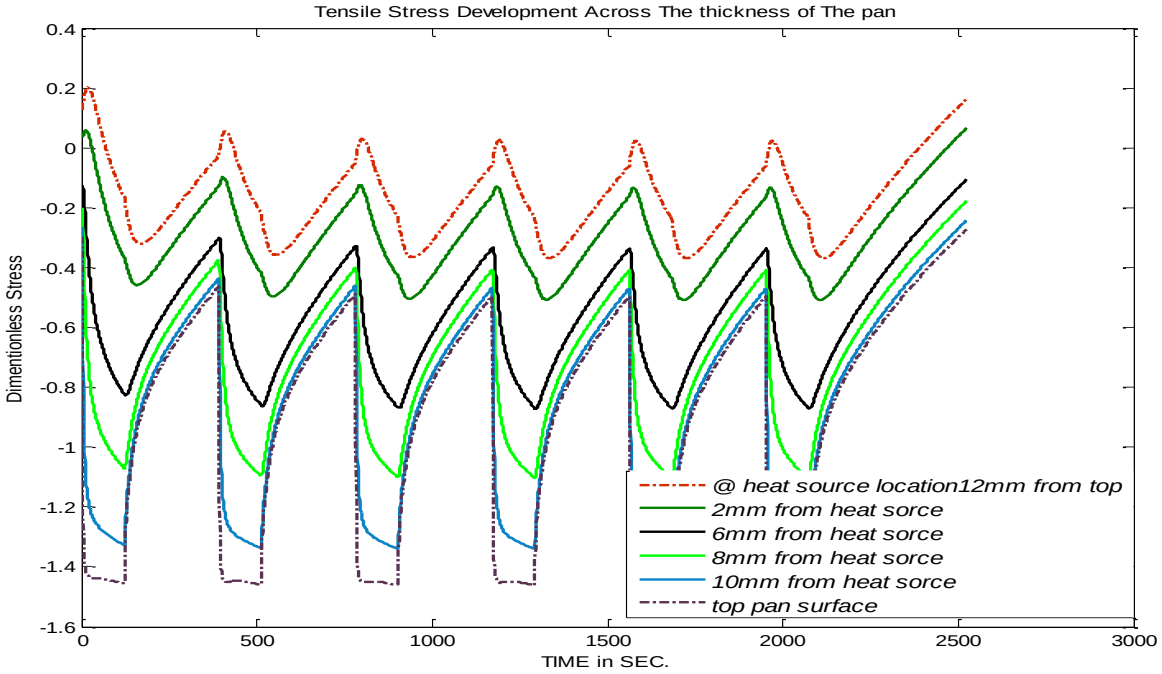

Figure 4-14: *Stress variation due to sudden cooling of the top surface during injera baking.*

During baking period the top surface cools down and needs to contract and the wormer bottom surface is in expansion and resists this contraction so the top surface becomes in tension. Since ceramics are week in there tensile strength the cyclic need to contract at the top surface due to cyclic baking eventually cause weakening of the top tine layer and forces it to separate from the main body. In addition to this the temperature gradients that occur radially also produce stress; hence more radial difference in expansion that may contribute to the failure of the ceramic body.

Form the figure 4.14 it can be seen that based on the thermo physical properties of the ceramic body used for the simulation the temperature gradient and thus the thermal stress development is greater if the mitad is thicker, and a body with smaller thickness cannot create significant temperature gradient to cause failure due to thermal stress gradient across the body. So the benefit of using a ceramic mitad with smaller thickness would be; in one hand it reduces the power rating of the stove and improves its performance and in the other hand it also protects failure due to thermal stress development that would cause failure if the mitad were thicker, i.e. reducing the thickness also helps to increase the reliability of the bake ware.

CHAPTER FIVE

EXPERMENTAL INVESTIGATION OF THE THERMAL AND MECHANICAL PERFORMANCE OF THE STOVE

5.1 The Ceramic Bake Ware and its Preparation for Baking

The ceramic bake ware manufactured was further prepared to provide a smooth nonstick baking surface. Two 1500 W resistor wires of type R09 are uniformly stretched and embedded in the grove for the purpose of resistance heating. The following figure shows the actual bake ware top and bottom surfaces.

Figure 5-1: *The bake ware (Mitad). Bottom of the bake ware with the built in grove (a) and top surface of the bake ware before smoothing (b)*

The Resistor wires are embedded in the bake ware and sealed with gypsum insulation and allowed to dry before assembling to the casing and body of the stove this is seen in figure 5.2.

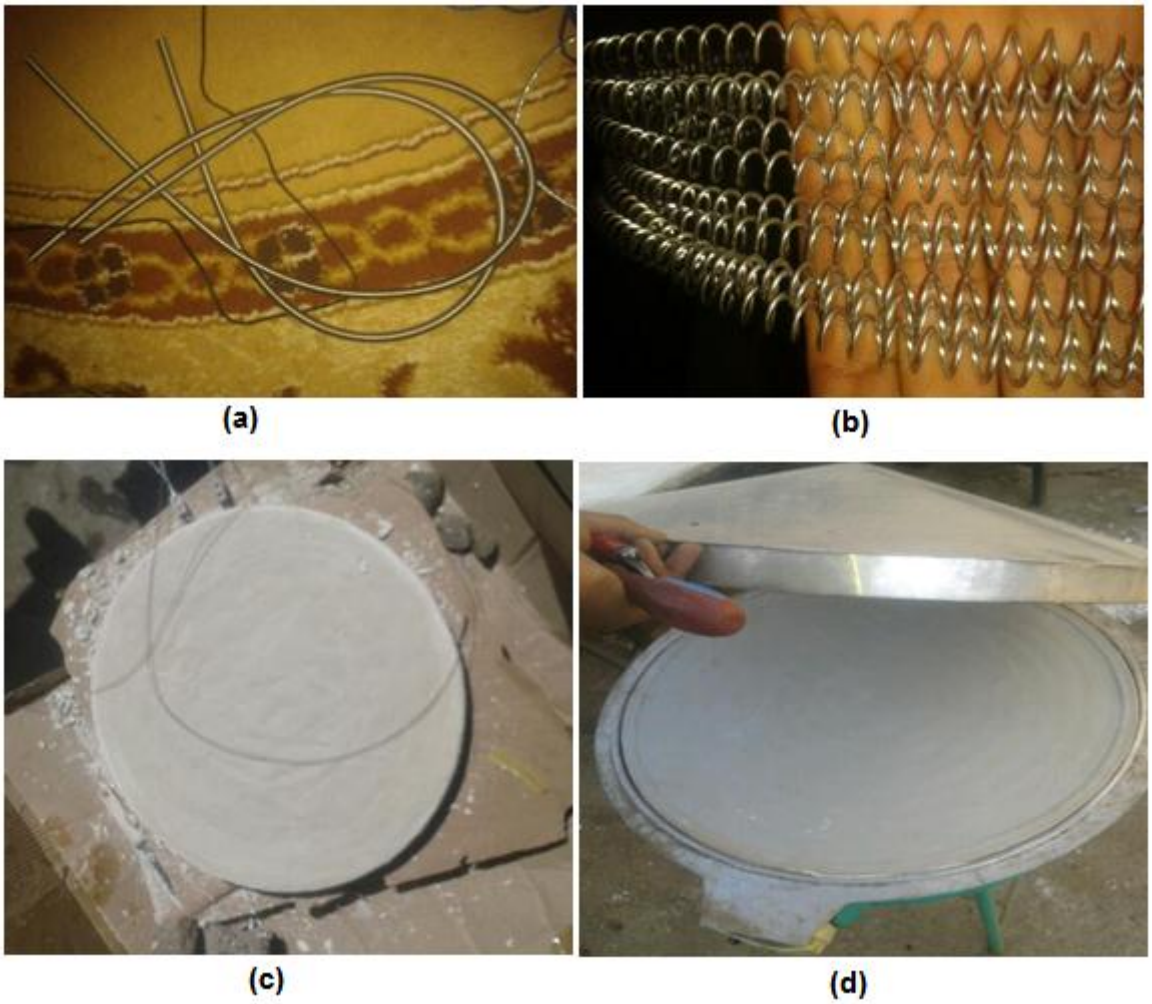

Figure 5-2: *The bake ware (Mitad) components. Resistance wire before stretching (a), uniform stretching of the resistor wire (b), Wire embedding and gypsum insulation (c) and final assembly with the stove casing (d).*

The green ware is made with a slip casting method which mainly contains alumina, feldspar, and quartz which was fired over 1220^{o}C to turn it in to ceramic; this process took 12 hours of stage by stage firing and 12 hours of cooling. Like most materials, ceramics conduct heat poorly relative to metals; but they retain heat well once they are hot, making them useful for slow cooking.

For high thermal conductivity of plates, the temperature of the plate surface varies from 110 to 140 degrees as thermal conductivity of the plate varies from 2 W/m.K to 50 W/m.K [15].

In this study, the ceramic bake wares are ordered and made in Tabor ceramic, HAWASA. And the research is on the bake ware procured from the Tabor ceramic private ltd.

5.2 Surface Preparation of the Bake Ware

Surface preparation of ceramic bake ware is required to create a no-stick top surface, previous researches and traditional techniques were used, as reported in [4]; Initially a layer of vegetable oil is putt on the bake ware surface and the bake ware was heated until the vegetable oil is burned and creating a black organic tar which filled in the rough surface of the bake ware. Then after the surface is smoothed and hardened, crushed a traditional oil seed ("gomenzer") and flax seed is burnt on the heated surface and the burning seeds are rubbed into the surface to create the final smooth no-stick coating[4]. After such preparation, the bake ware was tested for injera baking applications.

Figure 5-3: *Pretreatment of the bake ware before baking. Burning of gommenzer (powdered oil seed) on the surface of the bake ware (a) and the final smoothened and hardened surface (b)*

5.1 Dough preparation

The dough were prepared so that it contains 70 % moisture and 30% dry matter , to do this first the 2kg of Teff is gradually mixed with 5 litters of water in two stage ; one at the time of initial dough preparation and second at the time of "Habsit" preparation. The Habsit preparation stage gives the dough sufficient liquidity to be poured on to the baking surface. This is summarized in figure 5.4.

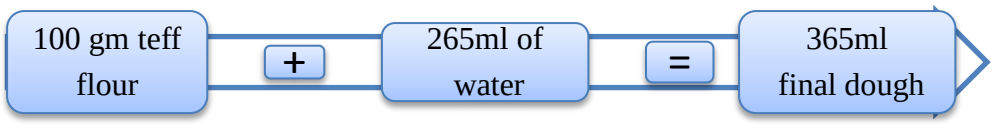

Figure 5-4:- *Dough preparation process*

This gives a net amount of 72.6% moisture content and 27.4 % Solid teff flour, the dough is then ready to be baked on the bake ware, and the prepared dough at the time of baking is as sown in figure 5.5.

Figure 5-5: *Dough ready to bake at the surface of the bake ware*

5.3 Experimental Test Equipments

The following instruments were used to collect data's during the heating up periods and baking times.

Infrared thermometer:- used to record the temperatures at the top of mitad, top of the cover, side of the stove and bottom wall of the stove, this data's were used to estimate the heat transfer coefficients during heating up and baking cycles in the simulation.[Appendix B].

Electric Multi Meter: - This was used to measure the current flow through the wire both during heat up time and cyclic baking times and the voltage available at the terminal [Appendix C].

Digital mass Balance: - this was used to measure the initial weight of the dough and the final weight of the product; injera. The weight of the paper and the cup were subtracted from the total weight seen in the picture. The mass of the dough was 497.5 gram and that of injera, final product was 416.6 gram.

Figure 5-6: *Temperature measurement instruments. Infrared thermometer (Left) and Multi -meter (Right).*

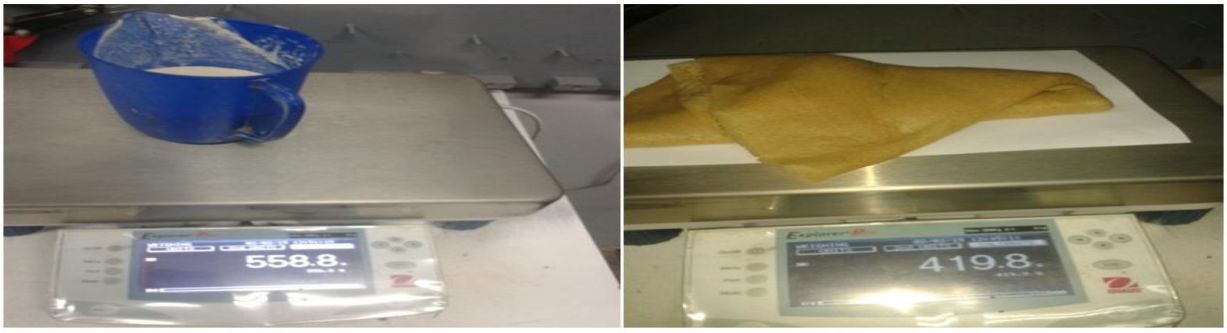

Figure 5-7: *Weighing instruments. The weight of dough (a) and the product injera (b)*

5.4 Heating up time, energy consumption and Surface Temperature of the Bake wares

The weight of the dough and injera were measured at four baking cycles and the results are as tabulated below.

Table 5-1: *Measured mass of injera, dough and mass loss of the final product*

Samples	Mass of dough in Gram	Mass of injera in gram	Moisture loss in gram
1	497.5	416.6	80.9
3	503.3	418.7	84.6
5	501.4	415.1	86.3
7	495.9	403.7	92.2
Average	499.525	413.525	85.975

The time taken to heat the bake ware to the temperature of baking was measured and found to be 20.5 minutes; the readings recorded with infrared thermometer are given in appendix D, the larger time taken is due to the increased size of the bake ware during manufacturing. The figure below shows the measured bake ware top surface temperature.

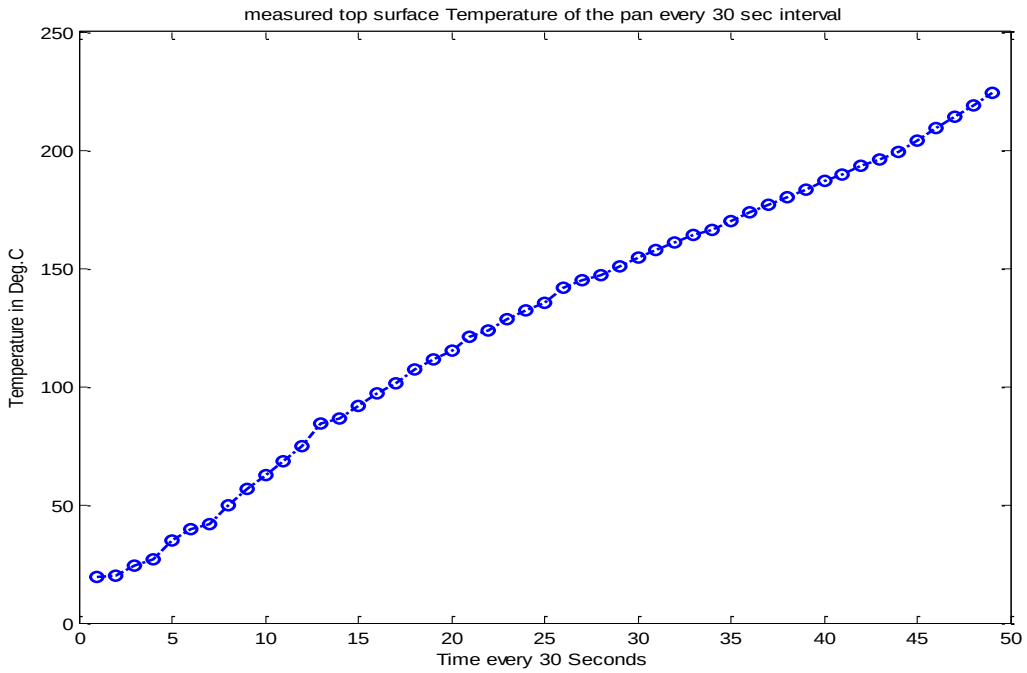

Figure 5-8: *Measured bake ware top surface temperature.*

5.5 Energy Consumption Calculation

The total heat up time and baking time energy consumption of the stove was calculated using the measured current flow as given in figure 5.9, the terminal voltage to the heating element was constant and taken as 220 V; but the current variation was measured in 30 seconds intervals and plotted and the resulting power dissipation in the heater were calculated at the times where the current were measured by using the current voltage and power relations derived from ohms law. The resulting power dissipation was plotted in figure 5.10 and the electrical energy consumption of the stove was numerically integrated from the power time curve.

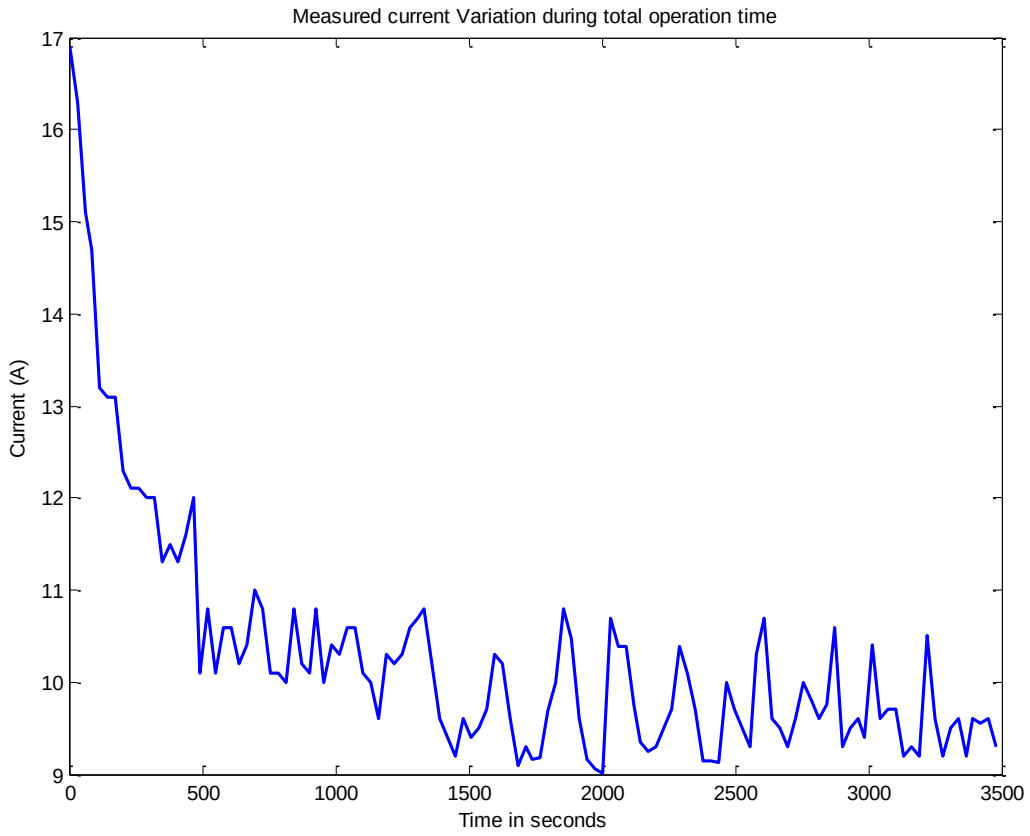

Figure 5-9: *The variation of current during the heat up and baking periods.*

The electrical Energy input to the stove is the voltage times the current times the time of heating.

$$dE = V * I(t) * \mathrm{d}t \qquad 5.1$$

The measured variation of current was used to determine the power supply and the electrical energy input to the stove. Using a constant terminal voltage of 220 V the variation of the power is as shown figure 5.10:

$$P_{(t)} = V * I(t) \qquad 5.2$$

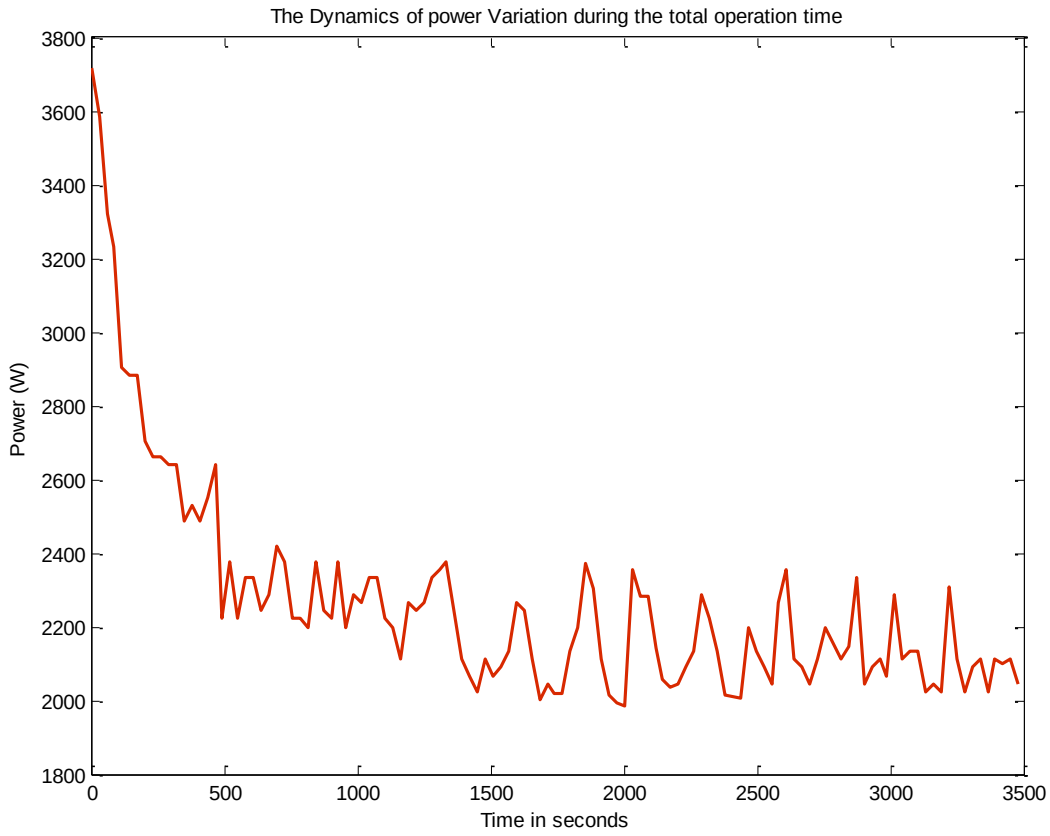

Figure 5-10: *The variation of power supply during the heat up and baking periods.*

Using trapezoidal rule numerical integration of the power time graph yields 8.2579Mj of total Electrical energy input to the stove throughout the operation.

$$Q_{total} = Q_{heat\ up} + Q_{baking} \qquad 5.3$$

The total electrical energy supply to the stove during heat up period is also numerically integrated for the first 20 minutes of heating up time and gives 3.0346Mj. The heat energy required by the current ceramic mitad to reach the temperature of baking as estimated by data's from previous researches and the weight of the current mitad is:

$$Q_{required} = mc_p * (T_h - T_c) \qquad 5.4$$

$$Q_{required} = 12.5 * 960 * (180 - 20) /= 1.92MJ$$

The heat loss from the mitad during heating up is then the difference of the electrical energy input during heat up period and the heat energy actually stored in the mitad:

$$Q_{loss} = 3.0346 - 1.92 = 1.1146MJ \qquad 5.5$$

5.5.1 Baking Energy Requirement

In this paper we measured the total energy requirement based on 10 cycles of injera baking. The mass of the dough before baking and the mass of the product injera were measured using Digital mass balance and the temperature of the product top surface were measured and used to calculate the actual energy of cooking. The time taken to bake one injera was measured and found to be 120 seconds, the average moisture change between the dough and the product injera was 0.086kg, and the initial mass of batter was 0.4135kg.So, for 10 baking cycles conducted, the total utilized energy was:

$$Q_{uf} = n_{cycle} * \{m_{inj} * c_{pin} * (T_{boil} - T_{init}) + \Delta m_{mo} * h_{fg} + \Delta m_{mo*\mathrm{Cpw}*(T_{bo}-T_{in})}\} \quad 5.4$$

$$=10*\{0.4135*3440.7*(100-20) +0.086*2.6*10^{6}+0.08596*4200*(100-20)\}$$

$$=3.663\mathrm{MJ}.$$

Or the utilized energy was 0.3663MJ/injera.

Where:-

Where; m_{inj} – is an average mass of the injera, kg;

C_{pinj} – average specific heat capacity of injera, J/kg k;

C_{pw}- specific heat capacity of water

T_{boil} – the product final temperature, ^{0}C;

M_{mo}– the moisture loss during baking, kg; and

h_{fg} – is the latent heat of water evaporation, J/kg.

Q_{uf}- the energy actually used for baking injera, J

The heat capacity of the product injera was taken from table 4.2; the evaporating temperature of water was taken as 100 ^{o} c.

The electrical Energy supplied during baking time is the difference of the total energy supply minus the energy supply during baking period.

$$E_{backing} = 8.2579mj - 3.0346mj = 5.2233Mj \quad 5.6$$

5.5.2 Utilized Energy Intensity and Total Energy Intensity

Energy intensity is the total amount of energy used to bake one kilogram of injera. It includes both the actual energy utilized in baking injera and the energy which is lost during baking, the average mass of the injera produced was 0.4135kg, and the total energy required to bake

10 injera was calculated as 5.2233Mj. The utilized energy intensity is the energy actually used to bake the injera (the energy utilized to change the liquid dough to the product injera) .The energy used per one injera is, the energy used to bake all the 10 injera divided by the mass of injera. This doesn't include the idle heating period.

$$\frac{E_{utilized}}{kg} = \frac{E_{used}}{mass\ of\ product} = \frac{3.663Mj}{10*0.4166kg} = 0.879MJ/kg \qquad 5.7$$

The heat up time taken for the bake ware was 20 to 23 minutes; i.e. 1200 seconds; the total time of operation is thus taking 20 minutes:

$$t_{total} = t_{\substack{heat \\ up}} + n * t_{baking+}(n-1) * t_{idle} \qquad 5.8$$

This gives the total time for 10 injera: it was observed that both the idle and baking periods took 2 minutes during field testing of the current mitad.

$$t_{total} = 1200 + 10 * 120 + 9 * 120 = 3480seconds$$

Where:-

Q_{uf-} the heat energy used for injera baking

$E_{heat\ up}$ – electrical energy consumption during heat up

E_{total}– total electrical energy consumption

n– Number of injera baked

Since electric to thermal conversion is 100 % efficient the E and Q terms and be used interchangeably

The overall total energy intensity including heat up period was calculated from the mass of the 10 injera and the total electrical energy input to the stove.

$$E_{\substack{intensity \\ total}} = \frac{E_{total}}{Q_{useful}} = \frac{8.2579MJ}{10*0.4135kg} = 1.996MJ/kg \qquad 5.9$$

The total energy intensity of the current ceramic bake ware is 0.2Mj/kg higher than that of the conventional clay mitad/bake ware/, this is mainly due to the increased thermal inertia of the current mitad due to an increased in thickness by 6mm from the conventional mitad/bake ware/.

5.6 Quality of Injera Baking and Reliability of the Bake Ware

To test the reliability of the ceramic bake ware for injera baking application, dough were prepared and baked on the surface when the surface temperature reaches 210 to 220^{o}C, and

the injera baked when the surface temperature was 210^{o}c produce a slightly burned bottom surface due to quick bottom crust formation and insufficient amounts of moisture were removed from the top surface as shown in figure 5.10 , but latter this problem was mitigated by using a top surface temperature of 150^{o}c, it takes 120 seconds to cook the injera to the desired quality. Figure 5.11 shows the top and bottom surfaces of the injera baked during the test. The quality of injera is as better as that cooked in clay bake ware. The ceramic bake ware was found to be non-stick and produced the same quality of injera as that of the conventional clay bake ware.

Figure 5-11: *Injera cooked at 210°C. (a) Top surface and (b) bottom surface*

Figure 5-12: *Injera baking process and the product (injera) at 150 ^{o}c surface temperatures.*

Due to the larger heat capacity of the current ceramic bake ware compared to the conventional clay bake ware; it losses much heat before an appreciable changes in top surface temperature; so the slight burning of the bottom surface as seen in figure 5.11 is due to the quicker crust formation before sufficient moisture is evaporated from the product body; to alleviate this problem the dough was poured at surface temperature of 150^{o}c and excellent qualities of the product injera were obtained as seen in figure 5.12.

Regarding the strength of the bake ware, a circumferential crack formed during manufacturing of the bake ware starts to propagate after 6 times heating and air cooling

cycles and three baking of injera and new cracks started to form for the subsequent baking cycles. The three main reasons of the weakening of the ceramic body are:

- The presence of residual stress during slip casting and firing times while manufacturing the ceramic body.
- The absence of a separate firing method and process suitable for the desired application of the bake ware; this ceramic bake ware was fired in the kiln with tiles and sanitary materials having different operation characteristics.
- The increased thickness; which is 2.6 cm creates temperature gradient across the body which then causes thermal stress to develop; and hence difference in expansion of parts across the thickness and radial directions.

Figure 5-13: *Shows the initial crack due to manufacturing and the propagation of new due to operation.*

5.7 Comparison of measured and simulated result

The top surface temperature obtained during experimental measurement was compared with the finite element simulation result and both are plotted on the same scale as shown in figure 5.6. In this paper only the heat up time is compared due to difficulties in reading the surface temperature variation of the mitad during baking periods.

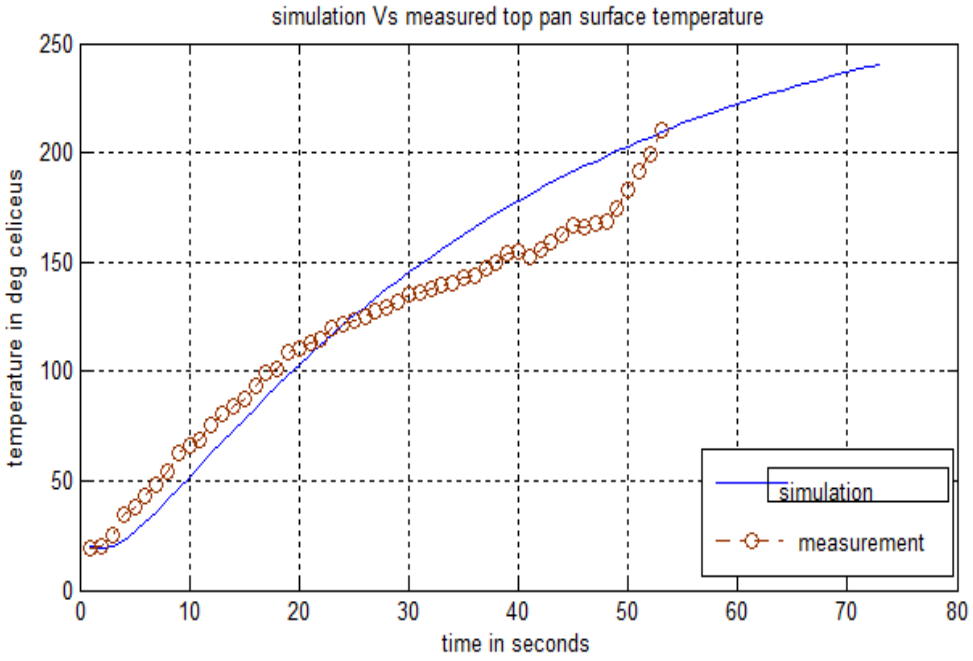

Figure 5-14: *Shows the experimental and simulation heat up time temperature history.*

The figure indicates there is a good agreement between the finite element simulation and the measured experimental result up to the first 20 minutes of heating and the deference becomes magnified at higher temperatures, this difference is mainly due to the higher rate of fresh air cooling effect at the surface while opening the cover for infrared temperature reading and at higher temperatures the cooling rate increases as the temperature difference increases.

The comparison of the total energy intensity shows 2.07Mj/kg from the simulation result and 1.996Mj/kg during experimental analysis, the difference is due the absence of exact thermo physical properties of the current ceramic mitad used for the test.

5.8 Results and Discussion

The results of the experiment shows, the ceramic bake ware with 2.6 cm thickness, 1.3 cm grove depth and 5 turns of double spiral grove having gypsum as bottom insulation reaches a baking temperature of 150^{o}c after 20.5 minutes of heating and gives 1.996Mj/kg of overall energy intensity. This value is 1.79Mj/kg for the conventional clay mitad. The difference is due to the increased thickness of the current mitad used for the test. It is seen that good qualities of injera were obtained at baking surface temperature of 147 to 150 ^{o}c; above this it was found to reduce the quality of the product both at the bottom and top surfaces.

Regarding the effectiveness and reliability of the stove while excellent baking quality of injera was observed for all cycles of baking, crack was observed at the surface of the bake

ware. The increased thickness of the new mitad and the presence of thicker edge boundaries produce temperature gradient across the thickness and the radial direction; which results in a thermal stress gradient in the body causing crack to commence and propagate at the top surface radial end locations.

The current ceramic bake ware takes longer time to reach the baking temperature compared to the conventional clay bake ware; this is mainly due to the higher thermal inertia of the ceramic mitad used for the test. Compared to the conventional clay bake ware the current ceramic bake ware produces quality injera at a surface temperature of 147 to 150^{o}C, this sows the ceramic mitad is able to bake injera at surface temperatures 30 to 50^{o}c lower than the surface temperature required by clay based stoves.

CHAPTER SIX

CONCLUSION AND RECOMENDATION

The parameters which affect the efficient and reliable operation of the bake ware and the stove were investigated and simulated, among this the heat capacity, thermal conductivity and the density are more significant in determining the heat flow characteristics ;the efficiency and the cooking quality of the product. The energy consumption for 10 cycles of injera baking were calculated from measured current flow and voltage values, the result indicates 1.996MJ/kg of total energy intensity ,which is comparably close to the value of the conventional clay mitad. The possibility of baking at a reduced surface temperature of 147 to 150^{o}C makes the ceramic bake ware preferable and the larger heat up time required becomes insignificant for larger cycles of baking; so it can be concluded that a ceramic bake ware can be a suitable alternative to the conventional clay bake ware for injera baking applications.

The thermal stress resistance of the bake ware were calculated analytically and tested during reliability cyclic baking test times, the original crack produced during slip casting were found to propagate after 10 cycles of baking and six heating and cooling cycles, a simulation on a reduced thickness of 12 mm were done and the analytical thermal stress values were lower than the breaking stress and the efficiency of baking was found to be 82 % for 20 baking cycles.

Recommendation

As it can be seen from this study a ceramic bake ware can be used for a substitute of clay for injera baking application and produces quality product (injera) at a reduced surface temperature; however the longer initial heat up and subsequent idle heating periods observed may results in poor efficiency compared to the conventional clay mitad with the same geometric and thermal boundary conditions.

Since the mitad sample were manufactured and fired with sanitary ceramic materials having different operating conditions, it was impossible to separately control the processing steps needed for its intended application. It can be recommended that mitad having the same ceramic composite but manufactured and fired separately can provide the desired thermo mechanical properties suitable for efficient and effective injera baking applications that could greatly enhance the performance of the conventional clay stove.

Based on the experimental and simulation results of the current ceramic bake ware the following conditions were recommended

- Sufficient insulation of the stove especially at the sides not only increase the efficiency of the operation but also keeps the edges of the bake ware warm enough to reduce damage to thermal stress and avoid stress concentration factors .
- Size reduction of the bake ware without loss of utility; reducing the thickness and diameter of the bake ware can have a synergetic effect both for the thermal stress resistance and efficiency of the bake ware.
- And a design which avoid restriction and allow free expansion at the sides of the stove can also improve thermal stress resistance of the ceramic bake ware.
- A ceramic body with the same body composition but fired at a controlled temperature and cooled gradually can also enhance the strength and performance of the bake ware.
- Care should be taken so that the bottom insulation shouldn't influence the upward heat flow from the heating element to the surface of the bake ware. If not the insulation material provides increased temperature gradient across the bake ware to reduce both the efficiency and longevity of the stove. Since the heating element (Nicrome wire) has high melting point($1400^{o}c$) it is possible to embed the wire during slip casting stage and can be fired together with the bake ware in the furnace. This can greatly increases the *structural strength*, the *thermal stress resistance* and *efficiency* of the bake ware.
- A detail study of the thermo physical properties of both mitads should be made in order to arrive at the optimum thermal and mechanical performance of the current ceramic mitad.

REFERENCE

1. Embassy of Japan in Ethiopia; Study on the Energy Sector in Ethiopia, September, 2008.

2. Zenebe Gebreegziabher, et.al (2010), Urban Energy Transition and Technology Adoption The Case of Tigrai, Northern Ethiopia, EfD DP 10-22.

3. Energy for rural development in Ethiopia, Proceedings of a National Policy Seminar 22nd –23rd November, 2000.

4. Awash Tekele, Experimental investigation on performance characteristics and efficiency of electric injera bake ware (mitad): November, 2011 Addis Abeba , Ethiopia

5. Nicrome 80 and other resistance alloys – technical and properties data, wiretron.com, wiretronic.inc

6. Gashaw Getenet; Heat transfer analysis during the process of injera baking by finite element method. et.al, November 2011, AAiT.

7. Prediction of specific heat of cereal flours: A quantitative empirical correlation, Go¨nu¨ l Kaletunc, The Ohio State University, 590 Woody Hayes Drive, Columbus, OH 43210, USA.

8. McGee, H., On Food and Cooking: The Science and Lore of the Kitchen, Simon and Schuster, New York, NY, 1984.

9. Horn, J., Cooking A to Z: The Complete Culinary Reference Source, New and Revised Edition, Cole Group, Santa Rosa, CA, 1997.

10. Lewis, R.W., Morgan, K., Thomas, H.R., Seetharamu, K.N., the Finite Element Method in Heat Transfer Analysis: John Wiley and Sons, Inc., 1996.

11. Luikov, A.V., Systems of Differential Equations of Heat and Mass Transfer in Capillary-Porous Bodies (review): International Journal of Heat and Mass Transfer, vol. 18, 1975, pp. 1-14

12. Incropera, F.P. and De Witt, D.P., Introduction to Heat Transfer, Second Edition, John Wiley & Sons, New York, NY, 1990.

13. Assefa Abate, "Transient heat transfer analysis of injera bake ware ("mitad") by finite element method", Unpublished thesis, Addis Ababa University, 2010.

14. David V. Hutton, Fundamentals of Finite Element Analysis, McGraw-Hill, 2004.

15.Luikov A.V.," Systems of Differential Equations of Heat and Mass Transfer in Capillary Porous Bodies (Review)", ht.J, Heat Mass Transfer, vol.18, pp. 1-14, 1973.

16.Rao S. S, The Finite Element Method in Engineering, Fourth Edition, Elsevier Science & Technology Books, USA, December 2004.

17.P.P.S.S. Pussepitiya and S.U. Adikary; su.Development of a High Thermal Shock Resistant Ceramic Body Suitable for Cookware Applications.

18.Ezana, N. and Van Buskirk, R. "Electric Enjera Cooker (Mogogo) Efficiency" Research Report: Energy Research and Training Division Department of Energy Ministry of Energy, Mines and Water Resources P.O. Box 5285 Asmara, Eritrea, October, 1996

19. Van Buskirk, R.,Haile,T. and Ezana,N. "The Effect of Clay and Iron Cooking Plates on Mogogo Efficiency and Energy Use: Experimental Results"

20. Van Buskirk, R.,Haile,T. and Ezana,N. "The Effect of Clay and Iron Cooking Plates on Mogogo Efficiency and Energy Use: Experimental Results"

21. W. D. KINGERYCeramics Division, Factors Affecting Thermal Stress Resistance of Ceramic Materials Department of Metallurgy, Massachusetts Institute of Technology, Cambridge, Massachusetts.

22. J. D. Bressan, M. M. Martins, and M. Vaz Jr ,Stress evaluation and thermal shock computation using the finite volume method ,Department of Mechanical Engineering, Centre for Technological Sciences, Santa Catarina State University, Joinville, Brazil.

22. Huang H., P. Lin and W. Zhou, "Moisture Transport and Diffusive Instability during Bread Baking, Unpublished M.Sc thesis, York University, June 9, 2006.

23. John H.Lienhard IV and John H.Lienhard.V; A Heat Transfer Text Book, Third edition. Phlogiston press, Cambridge Massachusets, 2004.

24.Joseph Irudyaraj, Food Processing Operations Modeling Design and Analysis, Marcel Dekker, Inc., New York, 2002.

25. Karin Thorvaldsen, Hans Janestad, "A Model for Simultaneous Heat, Water and Vapor Diffusion", Journal of Food Engineering, 40, 167-172, 1999.

26. Kenneth J. Valentas, Enrique Rothstein, and R. Paul Singh; Hand Book of Food Engineering Practice, CRC press, Newyork , 1997 ,

27. Krokida M. K., Michailidis P. A., Maroulis Z. M., and Saravacos G. D, "Literature Data of Thermal Conductivity of Food Stuffs", International Journal of Food Properties, 5(1), 63-111, 2002.

28. Krokida M. K., Zogzas N. P., and Maroulis Z. B., "Mass Transfer Coefficient in Food Processing: Compilation of Literature Data, International Journal of Food Properties, 4(3), 373-382, 2001.

28. Krokida M. K., Michailidis P. A, Maroulis Z. M, and Saravacos G. D, "Thermal Conductivity: Literature Data Compilation for Food Stuffs", International Journal of Food Properties, 4: 1,111- 137, 2001.

29. Van Buskirk, R.,Haile,T. and Ezana,N. **"**The Effect of Clay and Iron Cooking Plates on Mogogo Efficiency and Energy Use: Experimental Results".

30. Van der Pols, P., van der Vleuten, J., and Wouters, T. “Fuel-efficient injera stoves in Ethiopia”

31.MelikeSakin, FigenKaymak-Ertekin, CoskanIlicali, “Simultaneous Heat and Mass Simulation Applied to Convective Oven Cup Cake Baking”, Journal of Food Engineering, 83, 463–474, 2007.

32.Melike Sakin, FigenKaymak-Ertekin, CoskanIlicali, “Convection and Radiation Combined Surface Heat Transfer Coefficient in Baking Ovens’, Journal of Food Engineering, 94 344–349, 2009.

33. Michel Favre-Marinet and SedatTardu, Convective Heat Transfer. John Wiley & Sons, Inc.2009.

34.Nalaini D.Sabapathy,”Heat and Mass Transfer during Cooking of Chickpea Measurements and Computational Simulation”, Unpublished thesis, University of Saskatchewan, 2005.

35. www.zelaleminjera.com/products.html

36. Puri V. M. &Anantheswaranb R. C,"The Finite-Element Method in Food Processing: A Review”, Journal of Food Engineering, volume 19, pages 247-274, 1993.

37. Rao S. S, The Finite Element Method in Engineering, Fourth Edition, Elsevier Science & Technology Books, USA, December 2004.

38. Ressing H., M. Ressing, T. Durance, "Modeling the Mechanisms of Dough Puffing During Vacuum Microwave Drying Using the Finite Element Method”, Journal of Food Engineering, volume 82, page 498–508, 2007.

39. Rita M. Abalone, Analía G. Gastón1, and Miguel A. Lara,” Effect of Phase Change Criterion on the Prediction of Temperature Evolution During Food Drying” Mecanica Computational vol XXIV, 1135- 1147, Buenos Aires, Argentina, 2005.

40. Sablani S. S., Marcotte M., Baik O. D., and Castaigne F., Review Article: “Modeling of Simultaneous Heat and Water Transport in the Baking Process”,Lebensm.-Wiss.U. - Technol., 31, 201–209, 1998.

41. Sadik Kakac and YamanYener, Convective Heat Transfer, Second Edition, CRC Press, 1995, Tokyo.

42. Shaifur Rahman, Food Properties Handbook, second edition.CRC press, Washington, D.C, 1995.

43. Shahin Rafiee, Alireza Keyhani and Ali Mohammadi, “Soybean Seeds Mass Transfer Simulation during Drying Using Finite Element Method”, World Applied Sciences Journal 4 (2): 284-288, 2008.

44. SharanjeetDhawan and Sheo Kumar, “A Comparative Study of Numerical Techniques for

2D Transient Heat Conduction Equation using Finite Element Method", International Journal of Research and Reviews in Applied Sciences, Volume 1, Issue 1(October 2009).

45. Tong C.H., and Lund, D.B., "Microwave Heating of Baked Dough Products with Simultaneous Heat and Moisture Transfer", Journal of Food Engineering, 19,319-339, 1993.

46. Wu Y., Irudyaraj J., "Analysis of Heat, Mass and Pressure Transfer in Starch Based Food Systems", Journal of Food Engineering, 29, 399-414, 1996.

47. Young W. Kwon, The Finite Element Method Using Matlab, Second Edition, CRC press, 1997.

48. Yunus, A. Cengal, Heat Transfer: A practical Approach, McGraw-Hill series in Mechanical Engineering, USA, 1998.

49. Zanoni B., Peri C. and S. Pierucci, "A Study of the Bread-Baking Process I: A Phenomenological Model", Journal of Food Engineering, 19, No. 4, 389-398, 1993.

50. Zanoni B., Pierucci S., Peri C., "Study of the Bread Baking Process-II. Mathematical Modeling", Journal of Food Engineering, 23, 321-336, 1994.

51. Zhang J., Datta, A.K. "Mathematical Modeling of Bread Baking Process", Journal of Food Engineering, volume 75, pages 78–89, 2006.

52. ZhelevaIvanka and KambourovVesselka, "Identification of Heat and Mass Transfer Processes in Bread during Baking", Thermal Science: Vol. 9, No. 2, pp. 73-86, 2005.

APPENDEX

Appendix A:- Thermal properties of water during evaporation

T(^{0}C)	**ρ(kg/m^3)**	**C_p(J/kg.k)**	**K(w/m.k)**	**α(m^2/s)*10^7**	**V(m^2/s)*10^{-7}**	**Pr**	**β(k^{-1})**
100	958.3	4216	0.6796	1.681	2.94	1.75	0.000751
120	942.89	4245.63	0.682433	1.704	2.4896	1.4611	0.000858
127	937.5	4256	0.6836	1.713	2.332	1.36	0.000895

Appendix B:- Air properties

T(^{o}C)	ρ(kg/m^3)	C_p(J/kg.k)	K(w/m.k)	α(m^2/s)*10^{-3}	V(m^2/s)*10^{-7}	Pr	B*10^{-3}(k^{-1})
60	1.067	1.009	0.0285		18.9	0.709	3.0
80	1	1.009	0.0299		20.94	0.708	2.83
87.5	0.996	1.010	0.0305275	3.131	22.16	0.71	2.7739

Appendix C: - Average Temperature of the sides of the stove for heat loss calculation

No.	**Record points**	**T(^{o}C)**
1	Average side Temperature	63
2	Injera top surface Temperature	85
3	top cover temperature	44
4	bottom temperature	80
5	bake ware surface temperature	160

Appendix D: *Empirical equations used to compute thermal properties of food components. The equation works within temperature range of -40°C to 150°C*

Thermal Conductivity (*W/m·K)*

Protein	$k = 1.7881 \times$	10^{-1}	+	1.1958	×	$10-3t - 2.7178 \times 10-6t^2$
Fat	$k = 1.8071 \times$	10^{-1}	–	2.7604	×	$10-3t - 1.7749 \times 10-7t^2$
Carbohydrate	$k = 2.0141 \times$	10^{-1}	+	1.3874	×	$10-3t - 4.3312 \times 10-6t^2$
Fiber	$k = 1.8331 \times$	10^{-1}	+	1.2497	×	$10-3t - 3.1683 \times 10-6t^2$
Ash	$k = 3.2962 \times$	10^{-1}	+	1.4011	×	$10-3t - 2.9069 \times 10-6t^2$

Thermal diffusivity*(m2/s)*

Protein	$\alpha = 6.8714 \times$	10^{-8}	+	4.7578	×	$10-10t - 1.4646 \times 10-12t^2$
Fat	$\alpha = 9.8777 \times$	10^{-8}	–	1.2569	×	$10-10t - 3.8286 \times 10-14t^2$
Carbohydrate	$\alpha = 8.0842 \times$	10^{-8}	+	5.3052	×	$10-10t - 2.3218 \times 10-12t^2$
Fiber	$\alpha = 7.3976 \times$	10^{-8}	+	5.1902	×	$10-10t - 2.2202 \times 10-12t^2$
Ash	$\alpha = 1.2461 \times$	10^{-7}	+	3.7321	×	$10-10t - 1.2244 \times 10-12t^2$

Appendix E: *Continued*

Density ***(****kg/m3)*

Protein	$\rho = 1.3299 \times$	10^3	–	5.184	×	$10^{-1}t$
Fat	$\rho = 9.2559 \times$	10^2	–	4.1757	×	$10^{-1}t$
Carbohydrate	$\rho = 1.5991 \times$	10^3	–	3.1046	×	$10^{-1}t$
Fiber	$\rho = 1.3115 \times$	10^3	–	3.6589	×	$10^{-1}t$
Ash	$\rho = 2.4238 \times$	10^3	–	2.8063	×	$10^{-1}t$

Specific heat*J/(kg·K)*

Protein	$cp = 2.0082$	$\times 10^3$	+	1.2089	t	$- 1.3129 \times 10-3t^2$
Fat	$cp = 1.9842$	$\times 10^3$	+	1.4733	t	$- 4.8008 \times 10-3t^2$
Carbohydrate	$cp = 1.5488$	$\times 10^3$	+	1.9625	t	$- 5.9399 \times 10-3t^2$
Fiber	$cp = 1.8459$	$\times 10^3$	+	1.8306	t	$- 4.6509 \times 10-3t^2$
Ash	$cp = 1.0926$	$\times 10^3$	+	1.8896	t	$- 3.6817 \times 10-3t^2$

Appendix F: *Determination of specific heat of major components of injera*

major components	composition(%) x_j	specific heat(J/kg.k) xjcpj
carbohydrate	0.339	0.339(1.5488 +1.9625*10^(-3)T-5.9399*10^(-6)T^2)
protein	0.042	0.0042(2.0082+1.2089*10^(-3)T-1.3129*10^(-6)T^2)
fiber	0.017	0.017(1.8459+1.8306*10^(-3)T-4.6509*10^(-6)T^2)
ash	0.015	0.015(1.0926+1.8896*10^(-3)T-3.6817*10^(-6)T^2)
fat	0.006	0.006(1.9842+1.4733*10^(-3)T-4.8008*10^(-6)T^2)
moisture	0.581	0.581(4.1762-9.0864*10^(-5)-5.4731*10^(-6)T^2)

Appendix G: *Density of the major components of injera*

major components	composition(%) x_j	Density(kg/m3) ρi	xi/ρi
carbohydrate	0.339	1582.025	2.14*10^-4
protein	0.042	1301.388	3.23*10^-5
fiber	0.017	1291.376	1.32*10^-5
ash	0.015	2408.365	6.23*10^-6
fat	0.006	902.624	6.65*10^-6
moisture	0.581	985.987	5.89*10^-4
$\sum_{i=1}^{n} x_i \rho_i$=8.615*10^{-4}			

Appendix H: *Determination of the volume fraction of major components of injera*

components	composition(%)	Density(kg/m3)	xi/ρi	xi/ρi/(∑xiρi)
carbohydrate	0.339	1582.025	2.14*10^(-4)	0.248
Ash	0.015	2408.365	6.23*10^(-6)	0.00723
Fiber	0.017	1291.376	1.32*10^(-5)	0.015
Fat	0.006	902.624	6.65*10^(-6)	0.00772
Protien	0.042	1301.388	3.23*10^(-5)	0.03748
Moisture	0.581	985.987	5.89*10^(-4)	0.68353
∑xiρi=8.617*10^(-4)				

Appendix I: *Determination of thermal conductivity of major components for the parallel model*

components	εi	εiki
Carbohydrate	0.248	0.0499+3.4408*10^(-4)T-1.0741*10^(-6)T2
Ash	0.00723	2.3828*10^(-3)+1.0129*10^(-5)T-2.1014*10^(-8)T2
Fiber	0.015	2.7649*10^(-3)+1.8746*10^(-5)T-4.7525*10^(-8)T2
Fat	0.00772	1.3806*10^(-3)+2.1302*10^(-6)T-1.3697*10^(-9)T2
Protein	0.03748	6.37018*10^(-3)+4.4819*10^(-5)T-1.0186*10^(-7)T2
Moisture	0.68353	0.57109*Xw+1.7625*10^(-3)TXw+6.7036*10^(-7)T2Xw
K=0.0631+0.57109Xw+4.2999*10^(-3)T+1.7625*10^(-3)TXw-1.2459*10^(-6)T2+6.7036*10^(-6)T2Xw		

Appendix J: *Thermal conductivity of major components for the series model*

Components	composition	εi	ki	εi*ki
carbohydrate	0.339	0.24806	0.38466	0.6447
Ash	0.015	0.00723	0.49789	0.0145
Fiber	0.017	0.015	0.36346	0.0413
Fat	0.006	0.00772	0.29636	0.026
Protein	0.042	0.03748	0.35358	0.106
Moisture	0.581	0.68353	0.69775	0.9796
kseries=1/∑=εi*ki=0.5518w/m.k				

Appendix K: *MATLAB code for the simulation of the baking and heating process*

```
Clear all

Close all

%%%%%----------grid generation--------%%%%%%%

%%%%%----------bake ware properties and matricx generation-------%%%%%%%

kc=0.5;hc=15.45;rho=1900;cp=830;hcs=13.4;hcb=15.8;hboil=2000;

m=11;n=26;n1=23;Tsat=100;

alp=1./(rho*cp);

lx=0.3;ly=0.025;ly1=0.022;

hy=ly./(n-1);hx=lx./(m-1);

[x y]=ndgrid((0:lx/(m-1):lx),(0:ly/(n-1):ly));%/(n-1));

p=[x(:),y(:)];p1=p(1:m*n1,:);p2=p(m*(n1-1)+1:m*n,:);

t=[1,2,m+2;1,m+2,m+1];

t=kron(t,ones(m-1,1))+kron(ones(size(t)),(0:m-2)');

t=kron(t,ones(n-1,1))+kron(ones(size(t)),(0:n-2)'*m);

t1=[1,2,m+2;1,m+2,m+1];

t1=kron(t1,ones(m-1,1))+kron(ones(size(t1)),(0:m-2)');

t1=kron(t1,ones(n1-1,1))+kron(ones(size(t1)),(0:n1-2)'*m);

nt=size(t,1);nt1=size(t1,1);

tinj=zeros(nt-nt1,3);

t2=zeros(nt-nt1,3);

for i=n-1:n-1:size(t,1)

tinj(i-(n-2),:)=t(i-2,:);
```

```
tinj(i-(n-3),:)=t(i-1,:);

tinj(i-(n-4),:)=t(i,:);

end

t2(:,1)=nonzeros(tinj(:,1));

t2(:,2)=nonzeros(tinj(:,2));

t2(:,3)=nonzeros(tinj(:,3));

nnode=m*n;

botedge=[1:m-1;2:m]';

left=[1:m:m*(n1-2)+1;m+1:m:m*(n1-1)+1]';

left1=[m*(n1-1)+1:m:m*(n-2)+1;m*(n1-1)+2:m:m*(n-1)+1]';

right=[m:m:m*(n1-1);2*m:m:m*n1]';

right1=[m*n1:m:m*(n-1);m*n1+m:m:m*n]';

top=[m*(n1-1)+1:m*n1-1;m*(n1-1)+2:m*n1]';

top1=[m*(n-1)+1:m*n-1;m*(n-1)+2:m*n]';

sorclay=[11*m+1:12*m-1;11*m+2:12*m]';

source=[1:m-1;2:m]';

sorcenode=source(1,:);

matmass=rho*ly*pi*lx.^2;

Tinf=20;

Neuman1=unique(right);

Neuman2=unique(top);

egl=zeros(size(left,1),3);

Tn=zeros(n,m);
```

```
forjl=1:size(left,1)
egl(jl,:)=[(left(jl,1)),(left(jl,2)+1),(left(jl,2))];
end
Ta=20;
%%%%%%% matrix and force assembly for the whole domain%%%%%%%%%%
[k F cc ke]=assemb(p1,t1,kc,rho,cp,egl);
%%% matrix and vectors modification due to boundary conditions%%%
for j=1:size(right,1)
egt(j,:)=[(right(j,1)-1),(right(j,1)),(right(j,1)+m)];%%%right edge elements
k(egt(j,:),egt(j,:))=k(egt(j,:),egt(j,:))+...
 (2*pi*hcs*hy./(12))*[0 0 0;0 3*p(egt(j,2),1)+p(egt(j,3),1) p(egt(j,2),1)+p(egt(j,3),1);...
 0 3*p(egt(j,2),1)+p(egt(j,3),1) p(egt(j,2),1)+p(egt(j,3),1)];
F(egt(j,:)) = F(egt(j,:))+2*pi*Tinf*hcs*hy./(6)*[0;2*p(egt(j,2),1)+p(egt(j,3),1)...
    ;p(egt(j,2),1)+2*p(egt(j,3),1)];
end
%%%% left edge boundry condition %%%
forjl=1:size(left,1)
egl(jl,:)=[(left(jl,1)),(left(jl,2)+1),(left(jl,2))];
end
%%% bottom boundry condition nodes of heat source%%%
egs=zeros(size(source,1),3);
heat=egs;
forjb=1:size(source,1)   %%%%%% botom loss and stiffness modification
```

```
xend=p(source(end,:),:);

egs(jb,:)=[(source(jb,1)),(source(jb,2)),(source(jb,2)+m)];

   F(egs(jb,:)) = F(egs(jb,:))+2*pi*hcb*Tinf*hx./(6)*[2*p(egs(jb,1),1)+p(egs(jb,2),1)...

   ;p(egs(jb,1),1)+2*p(egs(jb,2),1);0];%%%%botom heat loss

k(egs(jb,:),egs(jb,:))=k(egs(jb,:),egs(jb,:))+...

 (2*pi*hcb*hx./(12))*[3*p(source(jb,1),1)+p(source(jb,2),1)
p(source(jb,1),1)+p(source(jb,2),1) 0;...

 p(source(jb,1),1)+p(source(jb,2),1) 3*p(source(jb,2),1)+p(source(jb,1),1) 0;0 0 0];

end

ppower=zeros(length(sorclay),3);

%sorclay=source;

Ff=F;kcook=k;

%[K2,F2]=injbake ware(k,F,kc,top,Tsat,hboil,hx,p,t,m,n);

%K2=KK;F2=FF;

%%top boundry for heat up%%%

forjt=1:size(top,1)

egtt(jt,:)=[(top(jt,1)-m),top(jt,2),top(jt,1)];

   F(egtt(jt,:)) = F(egtt(jt,:))+2*pi*Tinf*hc*hx./(6)*[0;2*p(egtt(jt,2),1)+p(egtt(jt,3),1)...

      ;p(egtt(jt,2),1)+2*p(egtt(jt,3),1)]; %%% ...

k(egtt(jt,:),egtt(jt,:))=k(egtt(jt,:),egtt(jt,:))+hx*...

 (2*pi*hc./(12))*[0 0 0;0 (3*p(egtt(jt,2),1)+p(egtt(jt,3),1)) (p(egtt(jt,2),1)+p(egtt(jt,3),1));...

  0 (p(egtt(jt,2),1)+p(egtt(jt,3),1)) (3*p(egtt(jt,2),1)+p(egtt(jt,3),1))];

end
```

```
Kk=k;

%Kk=k;Ff=F;

%%%%%%%%%%--------injera properties & matrices------%%%%%%%%%%%

hboil=2000;hm=0.5;rhoinj=1160.55;lamda=2256970;

cpinj=3650.075;kinj=0.6501;sigma=0.01;D=0.288*10.^(-4);

Moisto=0.73;Moistinf=0.25;hinj=8;Tinf=20;%er=0.3;

%n2=4;

Tme=1500;dt=1;Nt=Tme./dt;

fdt=zeros(size(p,1),Nt);

teta=1;

T=zeros(size(p,1),10);

T(:,1)=20;

leng=sum(2*pi*p(1:m),1);

leng=sum(leng);

flux1=zeros(m,1);

Ttop=zeros(m-1,Nt);Ttop1=zeros(m-1,10);

Ttop(:,1)=23;Ttop1(:,1)=20;

Tc=20;

TT=zeros(m*(n-n1),Nt);

TT(:,1)=23;

%Cbake ware=cc(1:m)

%%%%transient temperature computation

I(1)=22;
```

```
POWER(1)=(220.^2)./I(1);alphat=0.0004;Resistance(1)=220./I(1);

cycle=0;ncycle=6;theat=490;tbake=150;tidle=100;

it=1;

whileTc<200

it=it+1;

Twire=mean(T(sorclay(:,1),it-1));

I(it)=I(1)*(1+alphat*((Twire)-20));

Resistance(it)=220./I(it);

POWER(it)=(220.^2)./(I(it));

%sorclay=source;

forjbb=1:size(sorclay,1)%%%%% heat source at bottom nodes.

xend=p(m,1);

count=m-jbb;

    egbs(jbb,:)=[(sorclay(jbb,1)),(sorclay(jbb,2)+m),(sorclay(jbb,1)+m)];

  F(egbs(jbb,:)) =
Qg2(p(egbs(jbb,:),:),xend,alp,hx,POWER(it));%%%P(p(egs(jbb,:),:),count);...

ppower(jbb,:)=Qg2(p(egbs(jbb,:),:),xend,alp,hx,POWER(it)); %Qg(p(egs(jbb,:),:),xend,alp);

end

nn=(cc-((1-teta)*dt*Kk));

mm=(cc+(teta*dt*Kk));Fsol=F;

Fn=teta*dt*Fsol+nn*T(1:m*n1,it-1);

T(m*n1+1:m*(n),it)=23;

T(1:m*n1,it)=mm\Fn;
```

```
time(it)=(it-1)*dt;

Ttop(:,it)=T(m*(n1-1)+1:m*n1-1,it);

Tc=mean(Ttop(:,it));

Ttop1(:,it)=T(m*(n1-1)+m+1:m*n1+m-1,it);

end

Kevp=11.4*10.^(-5);Tevap=120;Ea=0.018*lamda;Rg=8314;

idletime=94;

while cycle<ncycle

cycle=cycle+1;

indx=it+(cycle-1)*(120+140);

for at=indx:indx+120;

Twire=mean(T(sorclay(:,1),at));

I(at+1)=I(1)*(1+alphat*((Twire)-20));

Resistance(at+1)=220./I(at+1);

POWER(at+1)=(220.^2)./(I(at+1));

%sorclay=source;

forjbb=1:size(sorclay,1)%%%%% heat source at bottom nodes.

xend=p(m,1);

count=m-jbb;

    egbs(jbb,:)=[(sorclay(jbb,1)),(sorclay(jbb,2)+m),(sorclay(jbb,1)+m)];

Ff(egbs(jbb,:)) =
Qg2(p(egbs(jbb,:),:),xend,alp,hx,POWER(at+1));%%%P(p(egs(jbb,:),:),count);...

ppower(jbb,:)=Qg2(p(egbs(jbb,:),:),xend,alp,hx,POWER(at+1));
%Qg(p(egs(jbb,:),:),xend,alp);
```

```
end

mi=0.73-(9.9*10^(-4))*(at-indx);

er=(at-indx)./(120);

fphase=er*exp((-Ea./Rg)*((1./T(m*(n-1)+6,at-1))-(1./94)));

fhase(at+1-indx)=fphase;

Revap=Kevp*mi.*fphase;

Qevap=lamda*rhoinj.*Revap;

[C21,C22,K22,F2]=thermatrix(rhoinj,cpinj,lamda,kinj,p,t,m,n,sigma,Revap,D);

%C21=C21(m*(n1-1)+1:m*n,m*(n1-1)+1:m*n);

bound2=right1;bound3=top1;

top2=top+m;

Tsat1=120;%(1./3)*(T(top(6,1)+m,at)+T(top(6,2)+m,at)+T(top(6,1),at));

[K2f,F2f]=thermboundry(top,bound3,bound2,F2,K22,(1-fhase(at+1-
indx))*hinj,p,t,m,n,hx,hy,Tinf,Tsat1,hboil,fphase);

%K2f=K2f(m*(n1-1)+1:m*n,m*(n1-1)+1:m*n);

%F2f=F2f(m*(n1-1)+1:m*n,1);

[K2,F22,C2]=superimposse(cc,C21,kcook,Ff,kc,K2f,F2f,n,m,n1);

     Tsat2=Tevap;%T(m*(n-1)+6,indx-1);

hcontact=2600;

    [Kn,Fn2]=injbake ware(K2,F22,kc,top,Tsat2,hcontact,hx,p,t,m,n1,fphase);

%Fn2(sorclay)=0;

nn=(C2-((1-teta)*dt*K2));

mm=(C2+(teta*dt*K2));Fsol=F22;
```

```
Fn=teta*dt*Fsol+nn*T(:,at);

T(:,at+1)=mm\Fn;

time(at+1)=(at)*dt;

Ttop(:,at+1)=T(m*(n1-1)+1:m*n1-1,at+1);

Ttop1(:,at+1)=T(m*(n-1)+1:m*n-1,at+1);

end

   Tc2=mean(Ttop(5,at+1));

idlet=at;

while Tc2<180

idlet=idlet+1;

Twire=mean(T(sorclay(:,1),idlet));

I(idlet+1)=I(1)*(1+alphat*((Twire)-20));

Resistance(idlet+1)=220./I(idlet+1);

POWER(idlet+1)=(220.^2)./(I(idlet+1));

%sorclay=source;

forjbb=1:size(sorclay,1)%%%%% heat source at bottom nodes.

xend=p(m,1);

count=m-jbb;

     egbs(jbb,:)=[(sorclay(jbb,1)),(sorclay(jbb,2)+m),(sorclay(jbb,1)+m)];

   F(egbs(jbb,:)) =
Qg2(p(egbs(jbb,:),:),xend,alp,hx,POWER(idlet+1));%%%P(p(egs(jbb,:),:),count);...

ppower(jbb,:)=Qg2(p(egbs(jbb,:),:),xend,alp,hx,POWER(idlet+1));
%Qg(p(egs(jbb,:),:),xend,alp);

end
```

```
nn=(cc-((1-teta)*dt*Kk));

mm=(cc+(teta*dt*Kk));Fsol=F;

Fn=teta*dt*Fsol+nn*T(1:m*n1,idlet);

T(m*n1+1:m*(n),idlet+1)=23;

T(1:m*n1,idlet+1)=mm\Fn;

time(idlet+1)=(idlet)*dt;

Ttop(:,idlet+1)=T(m*(n1-1)+1:m*n1-1,idlet+1);

Ttop1(:,idlet+1)=T(m*(n-1)+1:m*n-1,idlet+1);

    Tc2=mean(Ttop(:,idlet+1));

end

idletime=idlet-(at+1);

end

nodenum=zeros(m,n);

foriy=1:n

for ix=1:m

    i1=(iy-1)*n+ix;

nodenum(ix,iy)=i1;

end

end

cpwater=4200;

ncy=ncycle;

mbatter=0.497;mwater=0.084;

Qtotal=mean(POWER(1:end))*(it+ncy*120+(ncy-1)*(170));
```

```
Ecook=ncy*(mbatter*cpinj*(100-20)+mwater*lamda+mwater*cpwater*(100-20));

efficency=(Ecook./Qtotal)*100;

%%analytical claculation of thermal stress in the ceramic body

Tedge=T(13*m:m:m*n1,:);Tcent=T(12*m+1:m:m*(n1-
1)+1,:);Tmean=mean(T(12*m+1:m*n1,it));

miu=5.5*10^(-6);Eyong=386*10^(9);Stesion=206.8*10^(6);pois=0.21;

Scenter=1./(Stesion./(((1-pois)*Eyong*miu./(1-2*pois))*(T(m*(n1-1)+1:m*n1,it)-Tmean)));

Ssurface=1./(Stesion./((1-pois)*Eyong*miu./((1-2*pois))*(T(12*(m)+1:13*m,it)-Tmean)));

%assign temperature to grid points

tn=nodenum;

for index=1:m*n

tn(rem(index-1,m)+1,floor((index-1)/m)+1)=T(index,it);

end

Tnode=tn(:,1:n1)';

[xnode,ynode] = meshgrid(0:lx/(m-1):lx,0:ly1/(n1-1):ly1);

[Fr,Fz] = gradient(Tnode,hx,hy);

Fr = -kc*Fr;Fz = -kc*Fz;

[C h]=contourf(xnode,ynode,Tnode,20);

set(h,'ShowText','on','TextStep',get(h,'LevelStep')*2)

holdon,gridminor

xlabel('radial flux');ylabel('vertical flux');

quiver(xnode,ynode,Fr,Fz,2),colormaphot,holdoff,

pause
```

```
plot(time(1:end),T(m*n1-(7*m-5):m:end,1:end));grid minor;

title('cyclic baking temperatere profile across the baking disk and injera');

xlabel('time in seconds');

ylabel('Temperature in C');

pause

plot(time(it:it+90),T(m*n1+2:m*n1+m-2,it:it+90),time(it:it+90),T(m*(n1-1)+2:m*(n1-1)+m-2,it:it+90));grid minor;
```

Appendix L Components of the Stove used for the present test.

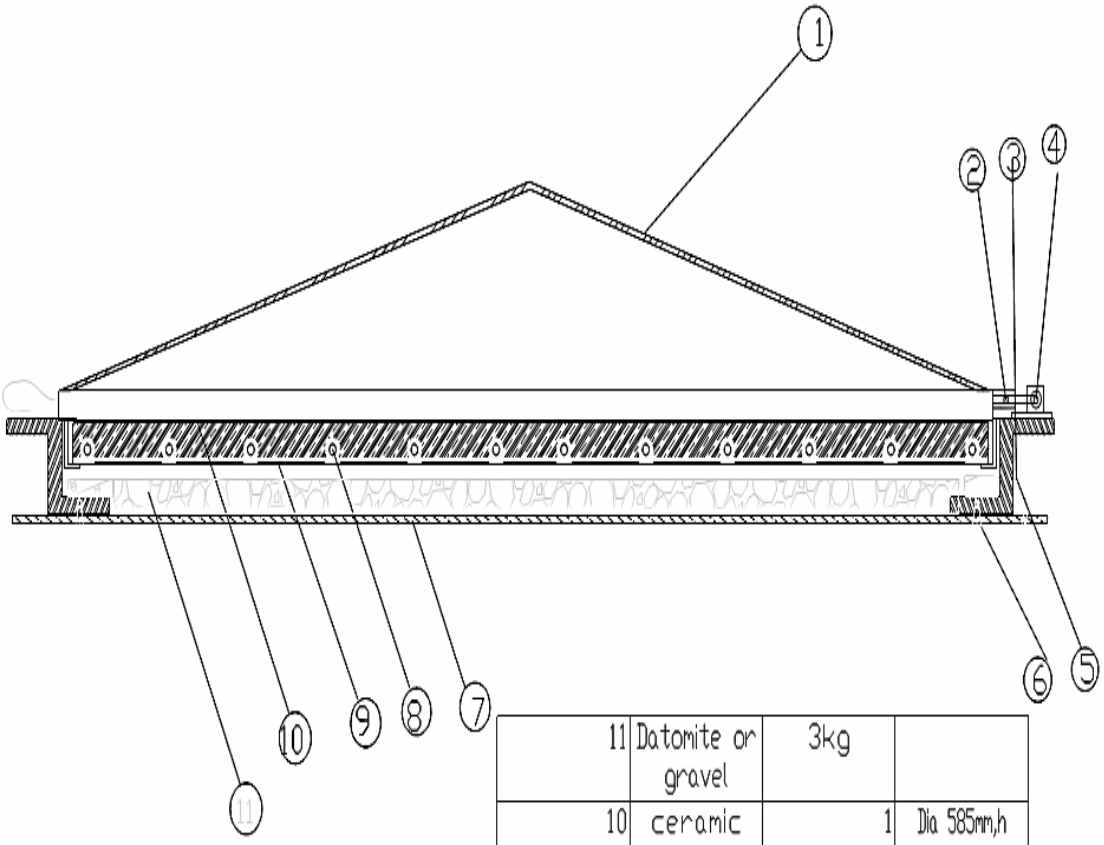

11	Datomite or gravel	3kg	
10	ceramic pan	1	Dia 585mm,h 26mm
9	gypsum insulation	double spiral groved	
8	risistance wire	2	R09
7	bottom casing		
6	screew		
5	stell side cover		
4	bracket		
3	link		
2	hing		
1	lid cover	1	D0.6m,H0.15m
ceramic electric stove			